Design Relations for the Wide-Band Waveguide Filter*

SEYMOUR B. COHN†, MEMBER, IRE

Summary—Design formulas are derived and presented graphically for a wide-band waveguide filter structure analyzed in a previous paper. The design procedure is outlined and a brief example given. Experiments indicate that the design cutoff frequencies and the infinite-attenuation frequency may be relied upon within one or two per cent.

THE WAVEGUIDE FILTER structure considered in this paper is shown in Fig. 1. This structure is most suitable for pass-band widths of the order of 1.5 to 1. The low-frequency cutoff f_c is provided by the natural cutoff of the waveguide, while the high-frequency cutoff f_1 is provided by the constrictions and cavities. The attenuation-versus-frequency response is sketched in Fig. 2. An accurate solution for this filter is given in a previous paper.[1] The formulas of that publication, however, are too unwieldly and contain too many parameters to enable simple application to a filter design problem. In this paper, it will be shown how the original equations may be simplified and represented graphically with very little loss of accuracy.

The Original Formulas

The following formulas for the image parameters are given in the paper on the analysis of this filter.[1]

$$y_I = \sqrt{y_{sc}y_{oc}} \tag{1}$$

$$\theta = \alpha + j\beta = 2\tanh^{-1}\sqrt{\frac{y_{oc}}{y_{sc}}} \tag{2}$$

where y_I is the image admittance of the filter, y_{sc} and y_{oc} the short- and open-circuit admittances of a half section, θ the image transfer function of one section, α the image attenuation function in nepers, and β the image phase constant in radians. All admittances are normalized with respect to the characteristic admittance of the rectangular-waveguide portions of the filter which are of height b and width a (Fig. 1). If a is held constant, the characteristic admittance of the guide is inversely proportional to b. Hence, the normalized characteristic admittance of the terminating line is equal to b/b_T. The half-section admittances are given by

$$y_{oc} = \frac{j}{\delta}\tan\left[\frac{\pi l'}{\lambda_g} + \tan^{-1}\left(\frac{\delta y_{oc'}}{j}\right)\right] \tag{3}$$

$$y_{sc} = \frac{j}{\delta}\tan\left[\frac{\pi l'}{\lambda_g} + \tan^{-1}\left(\frac{\delta y_{sc'}}{j}\right)\right] \tag{4}$$

where

$$y_{oc'} = j\tan\frac{\pi l}{\lambda_g}$$

$$+j\frac{2b}{\lambda_g}\left\{\frac{S_0(\delta)}{\pi^2} + \sum_{n>0}\left[\frac{\tanh\frac{n\pi lF}{b}}{F} - 1\right]\frac{\sin^2\pi n\delta}{n(\pi n\delta)^2}\right\} + j\epsilon_{oc} \tag{5}$$

$$y_{sc'} = -j\cot\frac{\pi l}{\lambda_g}$$

$$+j\frac{2b}{\lambda_g}\left\{\frac{S_0(\delta)}{\pi^2} + \sum_{n>0}\left[\frac{\coth\frac{n\pi lF}{b}}{F} - 1\right]\frac{\sin^2\pi n\delta}{n(\pi n\delta)^2}\right\} + j\epsilon_{sc} \tag{6}$$

$$F = \sqrt{1 - \left(\frac{b}{n\lambda_g}\right)^2} \tag{7}$$

$$\epsilon_{oc} \approx \epsilon_{sc} \approx \epsilon \approx -0.09b/\lambda_g \tag{8}$$

where δ is the ratio b'/b, and b', l', and l are dimensions shown in Fig. 1. λ_g is the guide wavelength of a uniform rectangular guide of width a. $S_o(\delta)$ is the Hahn function of zero order, which is tabulated by Whinnery and

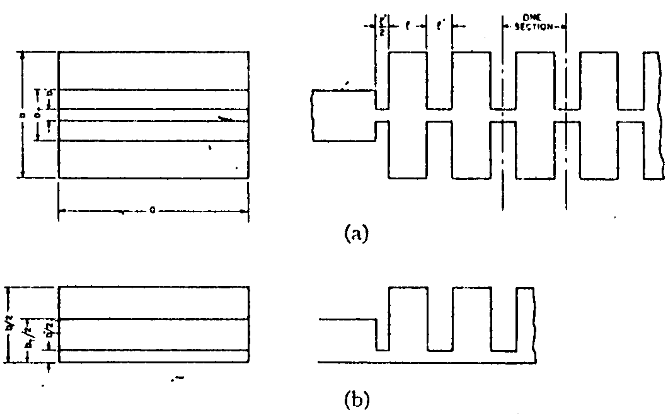

Fig. 1—The broad-band waveguide filter. The design information applies to both (a) and (b).

Jamieson.[2] Their value for $\delta = 0.05$ is in error, however, and should be $S_o(0.05) = 26.23$. For $\delta \leqq 0.15$, the following formula for $S_o(\delta)$ is within 0.4 per cent.

$$S_o(\delta) \approx \pi^2\left(\log_e\frac{1}{\delta} - 0.338\right). \tag{9}$$

The correction term of (8) is sufficiently accurate if δ is less than about 0.15, which is the case in the design of this type of filter. More accurate expressions for ϵ are given in (42) and (43) of footnote reference 1.

Formulas for the Filter Parameters

In the design of a filter, one must first decide where to place the cutoff and infinite-attenuation frequencies,

* Decimal classification: R386.1×R118. Original manuscript received by the Institute, September 20, 1949.
† Sperry Gyroscope Company, Great Neck, L. I., N. Y.
[1] S. B. Cohn, "Analysis of a wide-band waveguide filter," Proc. I.R.E., vol. 37, p. 651; June, 1949.

[2] J. R. Whinnery and H. W. Jamieson, "Equivalent circuits for discontinuities in transmission lines," Proc. I.R.E., vol. 32, pp. 98–115; February, 1944.

and what value of terminating resistance to use. For a waveguide filter section, these parameters are more conveniently expressed by the wavelengths λ_c, λ_{g1}, and $\lambda_{g\infty}$, and by the height b_T of the terminating guide. $\lambda_c(=2a)$ is the cutoff wavelength of a rectangular guide of width a, λ_{g1} the cutoff guide wavelength of the filter structure, and $\lambda_{g\infty}$ the infinite-rejection guide wavelength (Fig. 2). When a filter is being designed, it is necessary to obtain

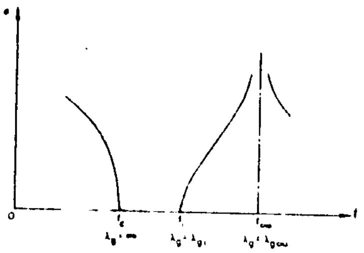

Fig. 2—Attenuation-versus-frequency response.

the filter dimensions which correspond to these given parameters. The difficulty of doing this by means of (1) through (8) is obvious. Hence it is necessary to change the form of these equations so that a straightforward design procedure will be possible. This is done below.

Let b_o be the terminating-guide height which would match the filter at f_c (i.e., for $\lambda_g \to \infty$). Then, by (1),

$$\lim_{\lambda_g \to \infty} (y_l)^2 = \left(\frac{b}{b_o}\right)^2 = \left[\lim y_{oc} \lim y_{sc}\right]_{\lambda_g \to \infty}.$$

When (3), (4), (5), and (6) are substituted and the limiting process carried out, one obtains[3]

$$\left(\frac{b}{b_o}\right)^2 = \left(\frac{l}{l+\delta l'}\right)\left\{1 + \frac{l'}{\delta l} + \frac{2b}{\pi^3 l} S_o(\delta) - \frac{2b}{\pi l}\sum_{n>0}\left[1 - \tanh\frac{n\pi l}{b}\right]\frac{\sin^2 \pi n\delta}{n(\pi n\delta)^2} + \frac{\lambda_g \epsilon}{\pi l}\right\}. \quad (10)$$

The actual height b_T of the terminating guide need not be equal to b_o. It will generally be chosen to give a perfect match at some point within the pass band, as explained later in the Design Procedure section.

Next, an implicit relation for the cutoff wavelength λ_{g1} will be obtained. This cutoff occurs when $y_{sc}=0$.[1] By means of (4) and (6), therefore, one obtains

$$\frac{\cot \pi \frac{l}{b}\frac{b}{\lambda_{g1}}}{\pi \frac{l}{b}\frac{b}{\lambda_{g1}}} = 2\frac{b}{l}\frac{S_o(\delta)}{\pi^3} + \frac{\tan \pi \frac{l'}{\lambda_{g1}}}{\pi\delta \frac{l}{b}\frac{b}{\lambda_{g1}}}$$

$$+ \frac{2b}{\pi l}\sum_{n>0}\left[\frac{\coth \frac{n\pi l}{b}\sqrt{1-(b/n\lambda_{g1})^2}}{\sqrt{1-(b/n\lambda_{g1})^2}} - 1\right]\frac{\sin^2 \pi n\delta}{n(\pi n\delta)^2}$$

$$+ \frac{\epsilon}{\pi \frac{l}{\lambda_{g1}}}. \quad (11)$$

The largest value of λ_{g1} which satisfies this equation yields the desired cutoff wavelength.

Lastly, an implicit relation for the infinite-attenuation wavelength will be derived. By (2), the attenuation α is infinite for $y_{oc}=y_{sc}$. When (3) and (4) are set equal, and (5) and (6) substituted, one obtains[3]

$$\csc\left(2\pi \frac{l}{b}\frac{b}{\lambda_{g\infty}}\right) = 2\frac{b}{\lambda_{g\infty}}\sum_{n>0}\frac{\operatorname{csch}\left[\frac{2\pi nl}{b}\sqrt{1-\left(\frac{b}{n\lambda_{g\infty}}\right)^2}\right]}{\sqrt{1-(b/n\lambda_{g\infty})^2}}\cdot\frac{\sin^2 \pi n\delta}{n(\pi n\delta)^2}. \quad (12)$$

Equations (10), (11), and (12) relate the critical wavelengths and the matching height to the filter dimensions, but they are still too complex for convenient use. It will now be shown how they may be put in graphical form with very little loss of accuracy.

The Design Graphs

Equation (12) contains three parameters, $b/\lambda_{g\infty}$, l/b, and δ. It is plotted in Fig. 3, where it is seen to be independent of δ for $l/b>0.2$. For $l/b<0.2$, linear interpolation between the curves for $\delta=0$ and 0.1 provides sufficient accuracy.

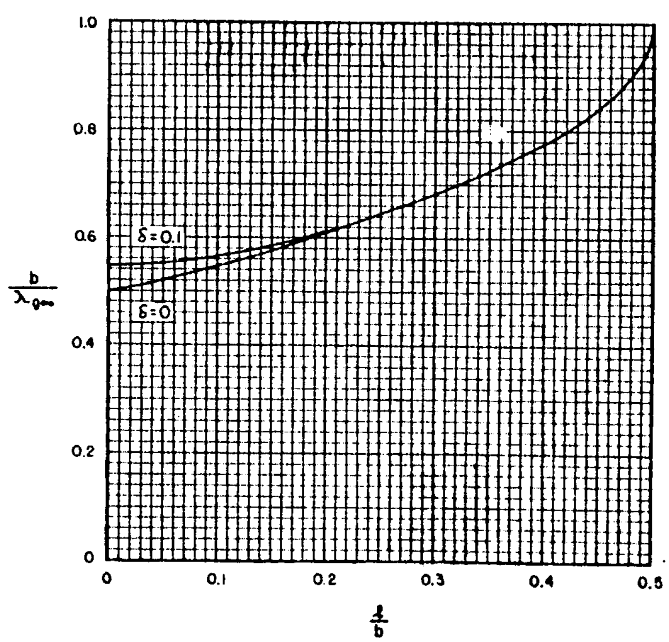

Fig. 3—Infinite-attenuation-wavelength curve.

Equation (10) has four parameters, b/b_o, l'/l, b/l, and δ. Fortunately, a greater error can be tolerated in b/b_o than in b/λ_{g1} or $b/\lambda_{g\infty}$, and hence several approximations may be made:

1. In practice, the product $\delta l'$ is generally less than one tenth as large as l. If the factor $l/(l+\delta l')$ is replaced

[3] These steps are performed in detail in "A Theoretical and Experimental Study of a Waveguide Filter Structure," by S. B. Cohn, Office of Naval Research, Cruft Laboratory, Harvard University, Report No. 39, April 25, 1948.

by unity, only a five per cent error in the image admittance match will result for $\delta l'$ as large as ten per cent of l. In any case where this error might be significant, the term $[1+\delta l'/l]^{1/2}$ may be used as a correction factor for the b_o value obtained from the simplified formula.

2. δ is usually equal to about one tenth or less. Because of this, and because the infinite series in (10) converges very quickly, the factor $(\sin \pi n\delta)^2/(\pi n\delta)^2$ may be set equal to unity with little error.

3. $\pi l'/\lambda_{g1}$ is usually small enough so that only a small error is introduced by setting $\tan \pi l'/\lambda_{g1}$ equal to $\pi l'/\lambda_{g1}$.

When these approximations are made in (10) and (11), and when the second resulting relation is subtracted from the first, one obtains

$$\frac{b_o/\lambda_{g1}}{b/\lambda_{g1}} = 1 + \frac{\cot \pi \dfrac{l}{b}\dfrac{b}{\lambda_{g1}}}{\pi \dfrac{l}{b}\dfrac{b}{\lambda_{g1}}} - \frac{2b}{\pi l}\sum_{n=1}^{\infty}\frac{1}{n}\left[\frac{\coth \dfrac{n\pi l}{b}\sqrt{1-(b/n\lambda_{g1})^2}}{\sqrt{1-(b/n\lambda_{g1})^2}} - \tan\frac{n\pi l}{b}\right]. \quad (13)$$

This has three parameters, b_o/λ_{g1}, b/λ_{g1}, and l/b. It is plotted in Fig. 4. The dashed curves are constant $\lambda_{g1}/\lambda_{g\infty}$ contours, which were calculated from Fig. 3 for $\delta=0$.

Equation (11) has four parameters, b/λ_{g1}, l/b, l'/λ_{g1}, and δ. Since only three independent parameters can be displayed on a single two dimensional graph, (11) will be divided into two separate relations, one of which may be directly calculated very simply, and the other of which may be reduced to three parameters and plotted. In (11) let

$$\frac{2S_o(\delta)}{\pi^3} + \frac{\tan \pi \dfrac{l'}{\lambda_{g1}}}{\pi\delta \dfrac{b}{\lambda_{g1}}} = G \quad (14)$$

where

$$G = \frac{\cot \pi \dfrac{l}{b}\dfrac{b}{\lambda_{g1}}}{\pi \dfrac{b}{\lambda_{g1}}} - \frac{2}{\pi}\sum_{n=1}^{\infty}\left\{\frac{\coth \dfrac{n\pi l}{b}\sqrt{1-\left(\dfrac{b}{n\lambda_{g1}}\right)^2}}{\sqrt{1-\left(\dfrac{b}{n\lambda_{g1}}\right)^2}} - 1\right\}\frac{\sin^2 \pi n\delta}{n(\pi n\delta)^2} + \frac{\epsilon}{\pi b/\lambda_{g1}}. \quad (15)$$

Equation (15) has four parameters—G, l/b, b/λ_{g1}, and δ—but δ may be eliminated as before by setting $(\sin \pi n\delta)^2/(\pi n\delta)^2$ equal to one. When this is done, only three parameters are left—G, l/b, and b/λ_{g1}. These are plotted in Fig. 5.

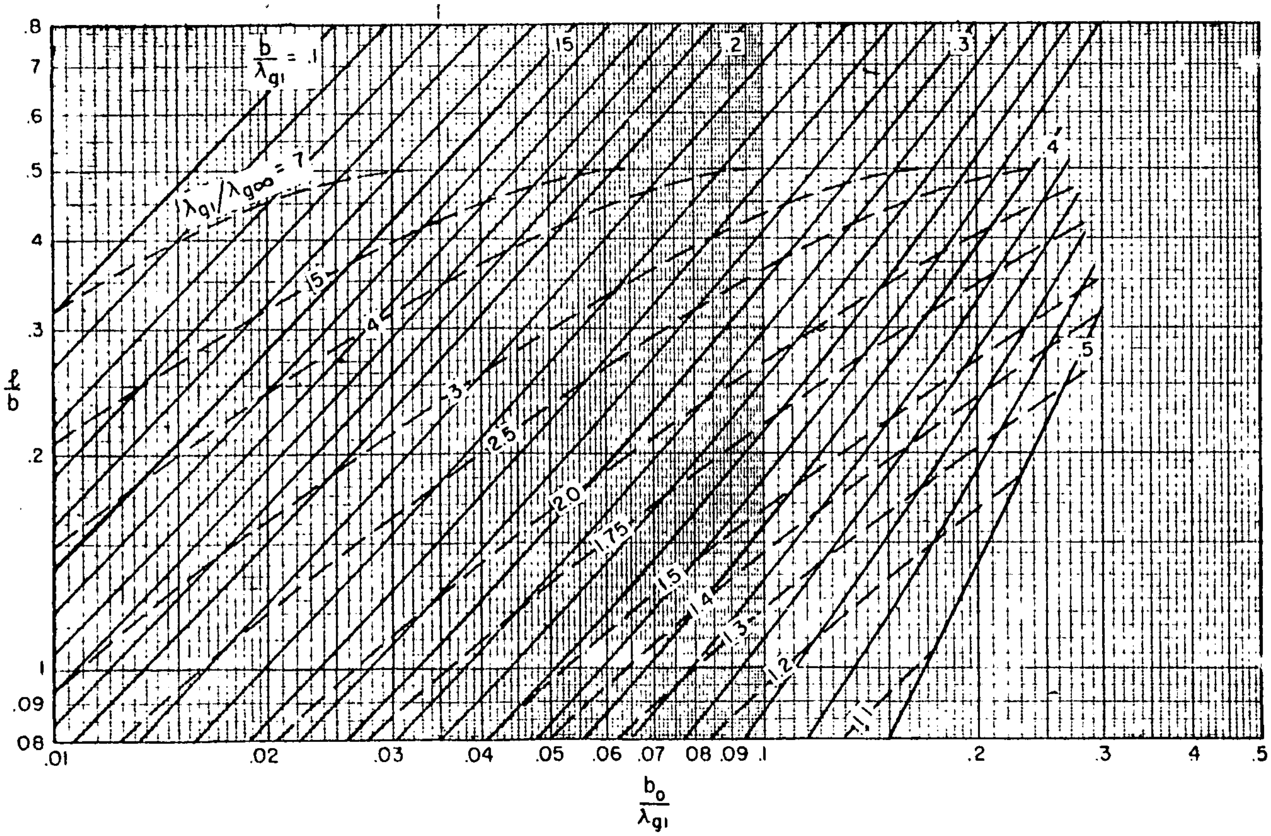

Fig. 4—Design graph giving the parameter b.

Declassified in Part - Sanitized Copy Approved for Release 2012/06/12 : CIA-RDP78-03535A000600010015-7

The parameters δ and l' are the last ones to be determined in carrying out a design. This may be conveniently done with (9) and (14) written in the following form

$$\tan \pi \frac{l'}{\lambda_{g1}} = \pi\delta \frac{b}{\lambda_{g1}}\left[G - \frac{2}{\pi} \log_e \frac{1}{\delta} + 0.215\right]. \quad (16)$$

After b/λ_{g1} and G have been found, a value of δ should be judiciously chosen, and then l' calculated by (16).

Design Procedure

The lower and upper cutoff frequencies and the infinite-attenuation frequencies are usually the given quantities in a filter-design problem. Corresponding to these three frequencies, the following wavelengths should be determined in the conventional manner: λ_c, λ_{g1}, and $\lambda_{g\infty}$. The width a of the structure is then given by $a = \lambda_c/2$. When the height b_T of the terminating guide has been chosen, a value of b_o may then be selected so that the image admittance of the filter will match the terminating impedance at some point in the pass band. In order to obtain such a match at λ_{g2}, the following approximate formula for b_o may be used:

$$b_o = b_T\sqrt{1 - (\lambda_{g1}/\lambda_{g2})^2}. \quad (17)$$

This follows from the approximate formula for the image admittance given in (24) of footnote reference 1. A fairly good over-all match occurs in the pass band if $b_o \approx 0.7\ b_T$. A much better match occurs if *transforming end sections* are used.[4]

[4] Radio Research Laboratory Staff, "Very High-Frequency Techniques," McGraw-Hill Book Co., New York, N. Y., Section 26-10; 1947.

Next, from Fig. 4, obtain l/b and b/λ_{g1} in terms of b_o/λ_{g1} and $\lambda_{g1}/\lambda_{g\infty}$. Then, from Fig. 5, obtain G in terms of l/b and b/λ_{g1}. Lastly, assume a value of δ and calculate l' from (16). If l'/b' is less than one half, or if l'/λ_{g1} is greater than $\lambda_{g1}/10$, a different value of δ should be tried.

Example: Let $a = 2.750$ inches ($f_c = 2145$ Mc), $b_T = b_o = 0.375$ inch, $f_1 = 3{,}000$ Mc ($\lambda_{g1} = 14.3$ cm $= 5.63$ inches), and $f_\infty = 3{,}500$ Mc ($\lambda_{g\infty} = 10.8$ cm). Hence $b_o/\lambda_{g1} = 0.0666$ and $\lambda_{g1}/\lambda_{g\infty} = 1.32$, and by Fig. 4, $l/b = 0.089$ and $b/\lambda_{g1} = 0.410$. Therefore, $b = 0.410 \times 5.63 = 2.31$ inches and $l = 0.089 \times 2.31 = 0.206$ inch. By Fig. 5, $G = 4.06$. Let $b' = 0.125$ inch, so that $\delta = b'/b = 0.125/2.31 = 0.0541$. By (16), $l' = 0.302$ inch.

A large number of sections may be used in order to have a sharp cutoff and high attenuation in the stop band. The sections need not all have the same f_∞ value, since dissimilar sections have almost identical image-admittance functions, if their cutoff frequencies and b_o values are the same.[1] Fig. 6(a) shows three sections each having the values of b_o, b', λ_c, and λ_{g1} of the above example. The infinite-attenuation frequencies are, however, from left to right 3,500, 4,500, and 5,500 Mc. By having sections with different f_∞ values, the insertion loss may be kept high in the passband, and also the spurious response of each section near $b/\lambda_g = 1$ will fall in the stop band of another section. A further discussion on the removal of spurious responses is given in the literature for a similar type of waveguide filter.[5]

[5] See pp. 734–736 of footnote reference 4.

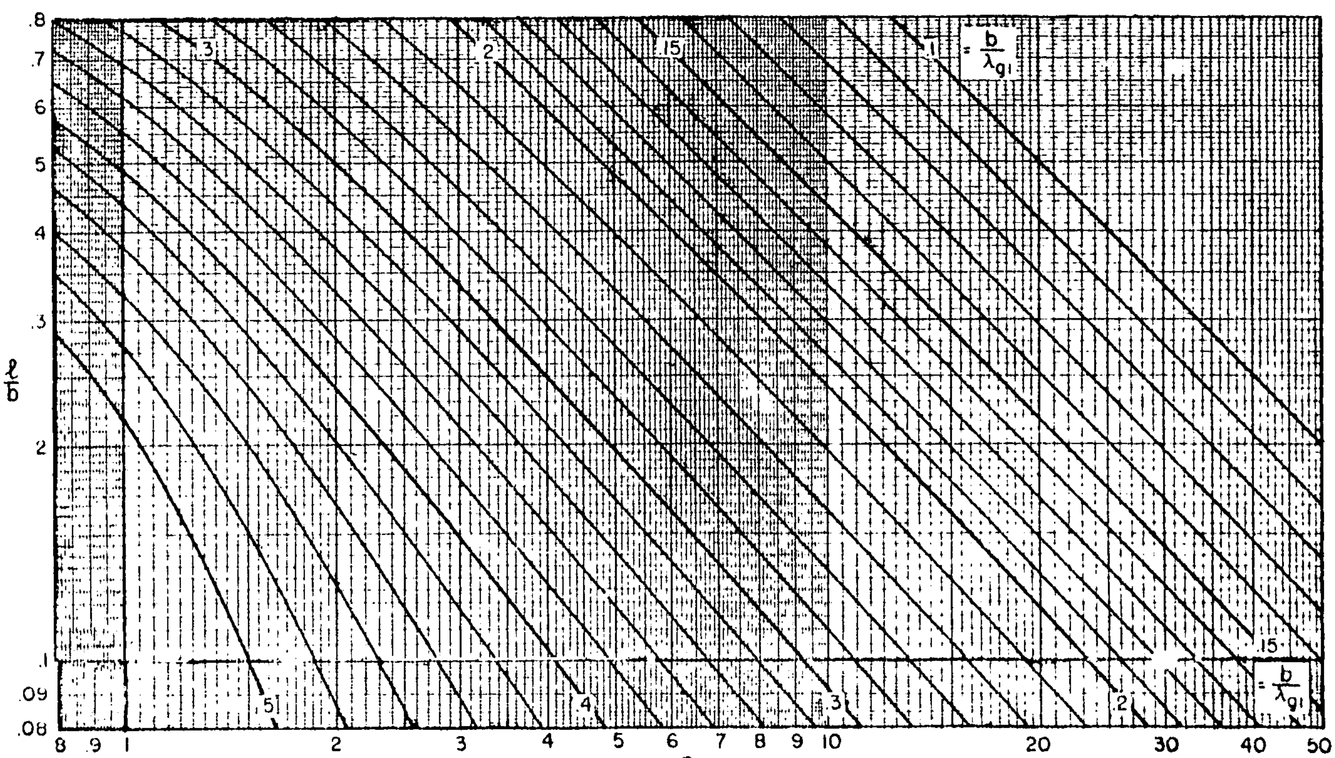

Fig. 5—Design graph giving the parameter G.

Before connecting the end sections to the terminating guide, the discontinuity capacitance due to the junction of heights b_t and b' must be compensated. This may be done to a close approximation by shortening the length of the constriction at each end of the filter from $l'/2$ to $l'/2 - \Delta l'$, where $\Delta l'$ is given by[3]

$$\Delta l' = \frac{b'}{\pi}\left(\log_e \frac{b_T}{b'} - 0.386\right). \tag{18}$$

Fig. 6(b) shows the assembled filter, after correction of the end constrictions.

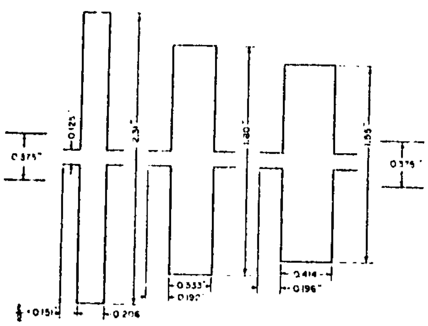

(a)

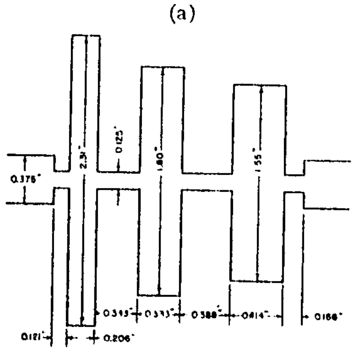

(b)

Fig. 6—A three-section waveguide filter, (a) before assembly and (b) after assembly. ($f_1 = 3{,}000$ Mc, $a = 2.75$ inches.)

Verification of Accuracy

Six individual sections terminating in 2.75×0.375-inch guide were constructed with a wide range of physical parameters. The f_1 cutoff frequencies were calculated from (11), except for filter number 5, and also from the design graphs. They were measured by two different methods which checked each other within 0.3 per cent.[4] The various cutoff-frequency values are listed in Table I. The data in the "Tests" column are averages for the two tests.

TABLE I

Values of f_1

Filter No.	Equation (11)	Design Curves	Tests
1	2,993 Mc	3,000 Mc	2,980 Mc
2	3,003	3,000	2,991
3	2,834	2,843	2,822
4	3,000	3,016	3,001
5		3,000	3,024
6	2,995	3,000	2,991

In each case, the spread of f_1 values is less than one per cent. The f_∞ values were calculated by (12) and also measured, and these too agree within one per cent. Since f_c is the natural cutoff frequency of the waveguide, which is known exactly, it need not be checked.

The approximations used in obtaining (13) and Fig. 4 cause an error in the image admittance of up to 5 or 10 per cent, which is generally too small to be of consequence. If the correction factor $[1+\delta l'/l]^{1/2}$ mentioned above in the Design Graph section is used, this error can be greatly reduced.

Acknowledgment

The writer wishes to acknowledge the many helpful suggestions of R. W. P. King and L. Brillouin toward the preparation of this paper.

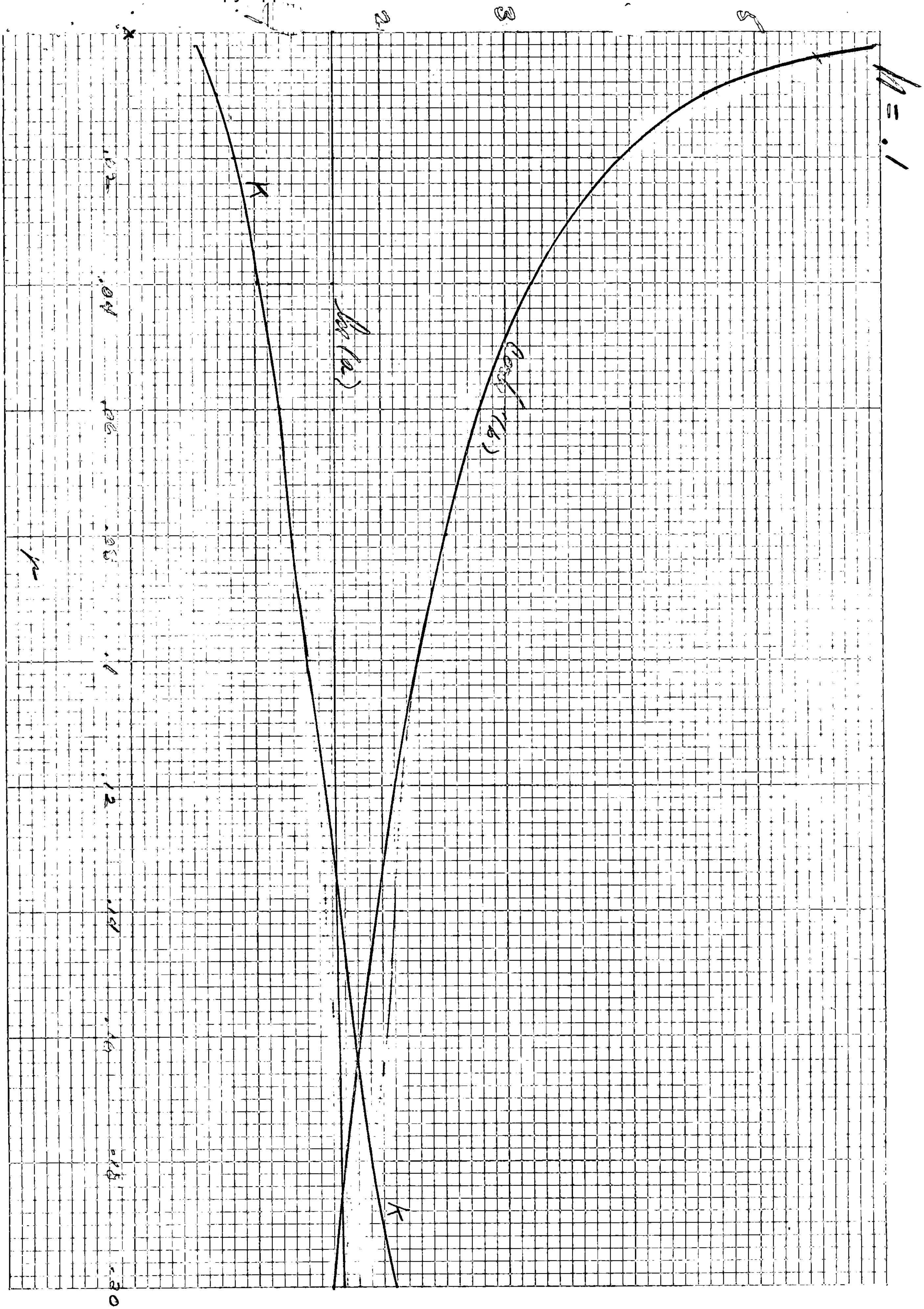

Declassified in Part - Sanitized Copy Approved for Release 2012/06/12 : CIA-RDP78-03535A000600010015-7

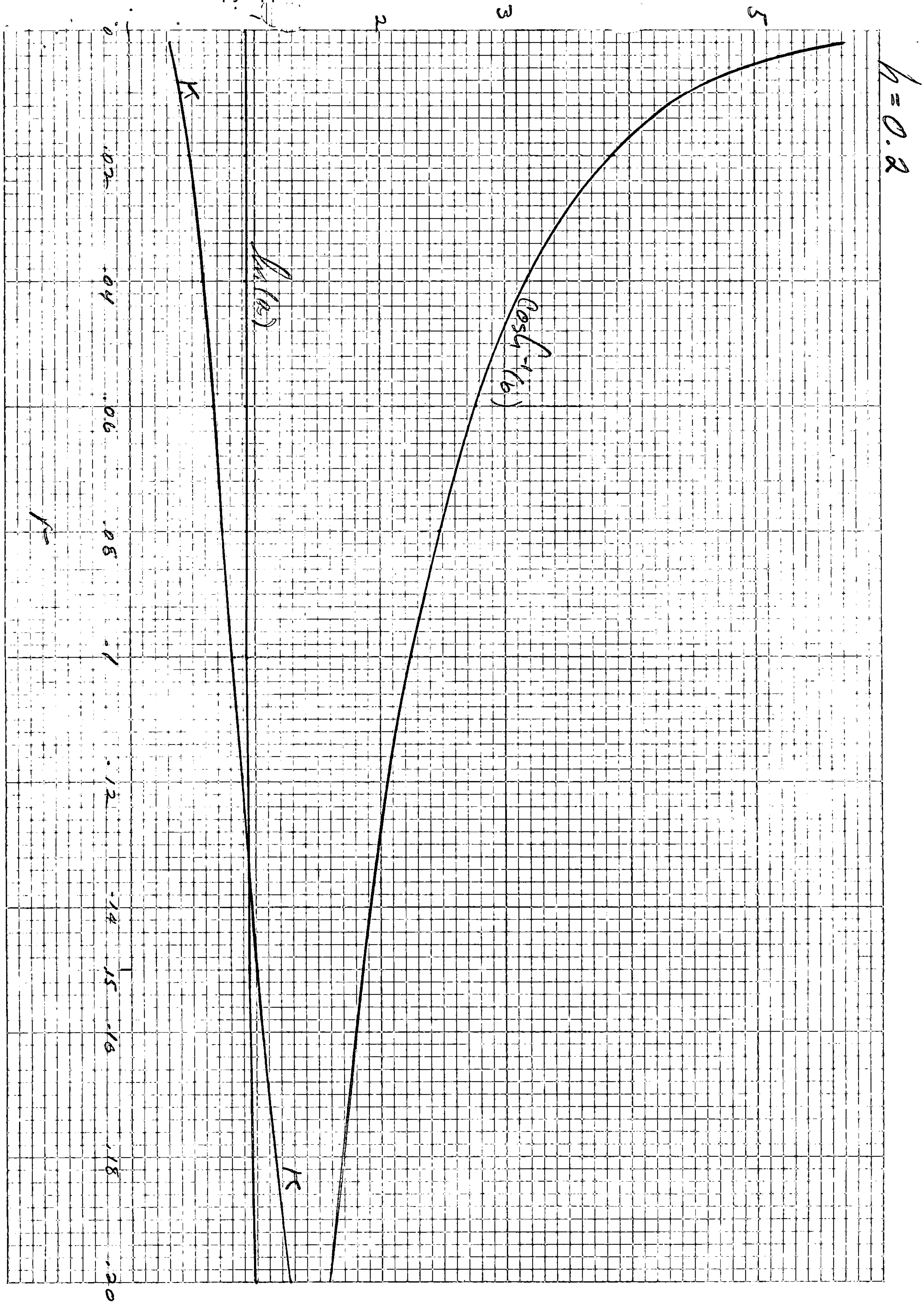

Declassified in Part - Sanitized Copy Approved for Release 2012/06/12 : CIA-RDP78-03535A000600010015-7

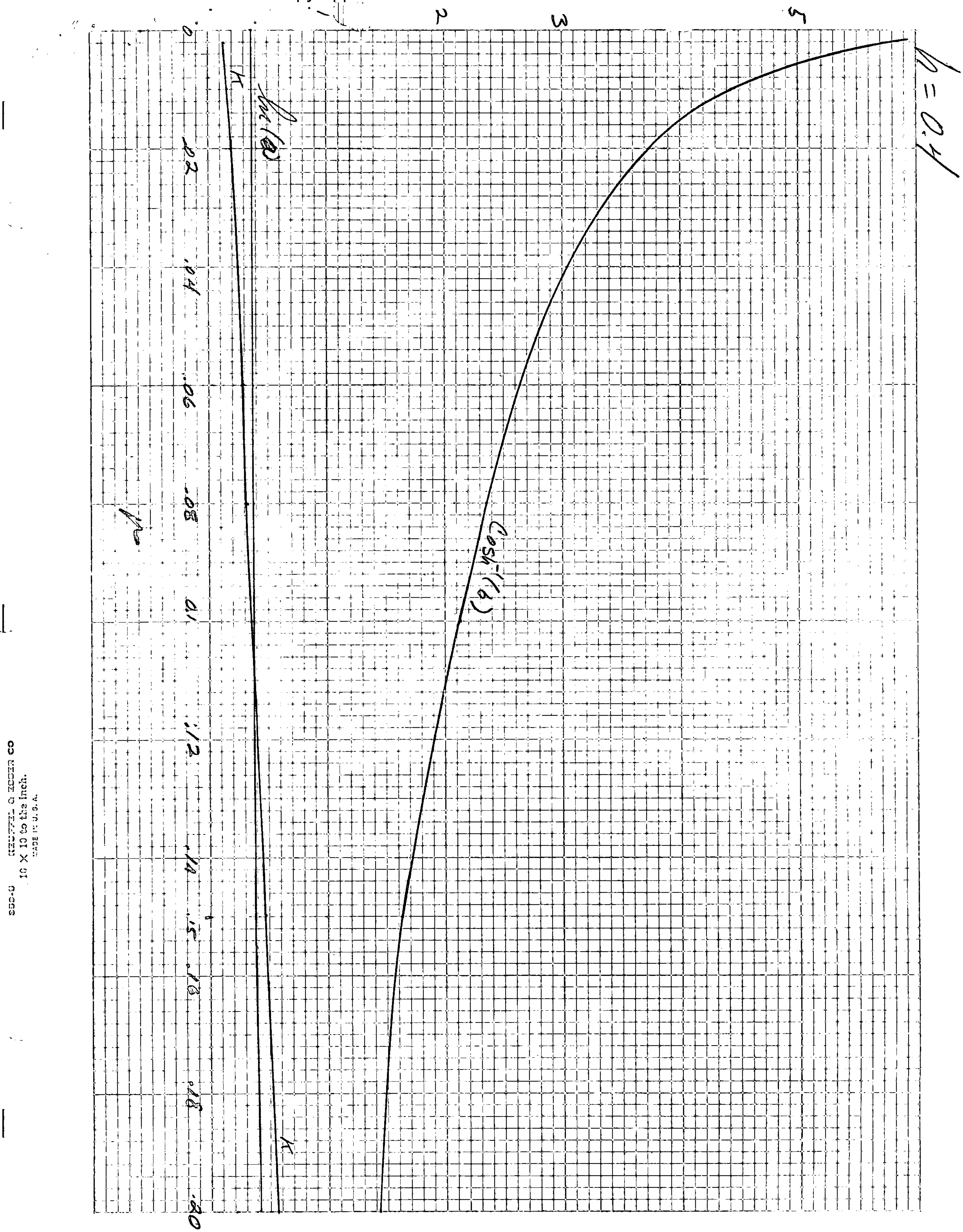

Declassified in Part - Sanitized Copy Approved for Release 2012/06/12 : CIA-RDP78-03535A000600010015-7

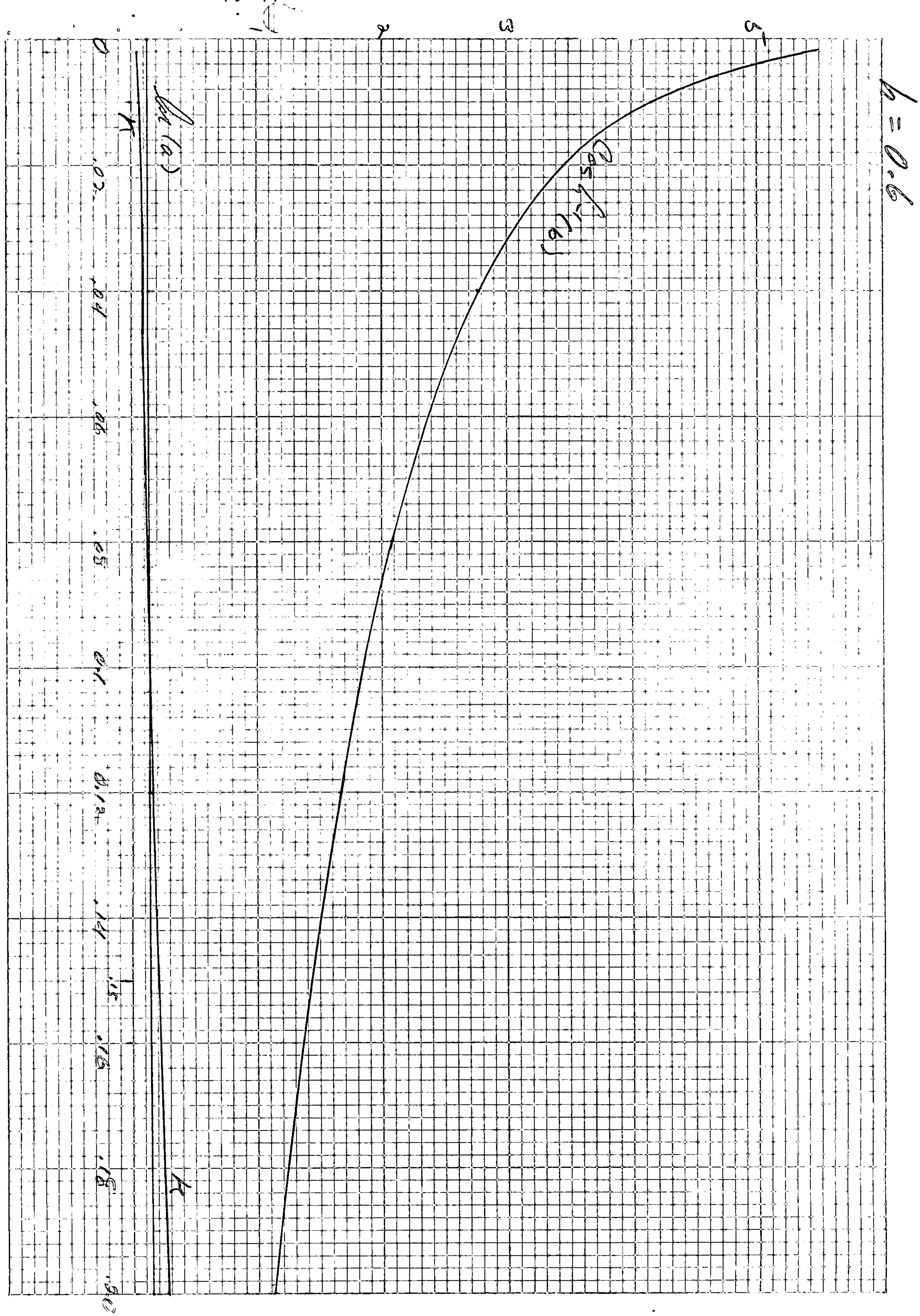

Declassified in Part - Sanitized Copy Approved for Release 2012/06/12 : CIA-RDP78-03535A000600010015-7

COAXIAL FILTER

$\boxed{2 - 3.2 \text{ kmc}}$

notation of Karakash & Mode

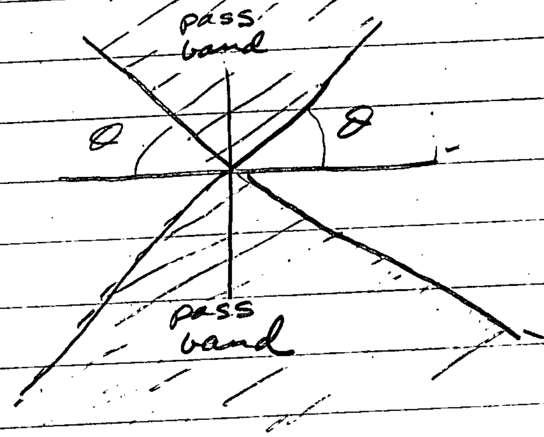

$\theta = 69.2^\circ = 1.207$ radian

$K = \cos\theta$

$\boxed{K = .356}$

$\dfrac{Z_I}{Z_0}\Big/_{f_0} = 2.44$

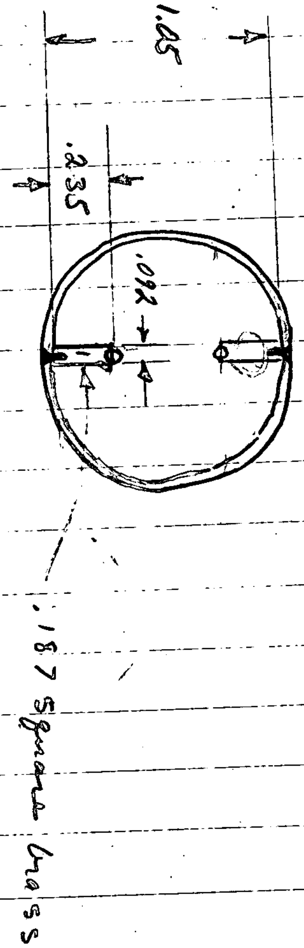

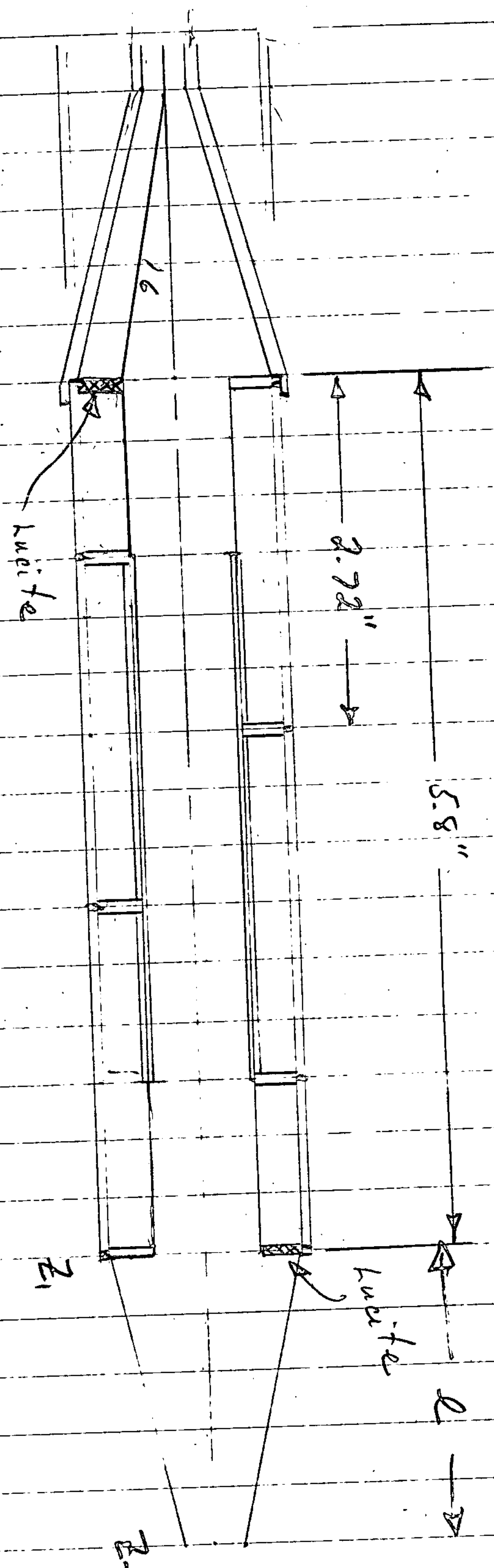

length of taper

$Z_2 = 50\Omega$

$Z_1 = 180\ \Omega$

$\frac{D}{d}\Big|_{Z_1} \doteq 20$

$\frac{l}{\lambda} \simeq \ln\left(\frac{180}{50}\right) = 1.27$

"Microwave Theory & Techniques"

$\lambda = 01 = \quad 19\ cm = 7''$

Reich, Ordung, Krauss, Skalnik P.191

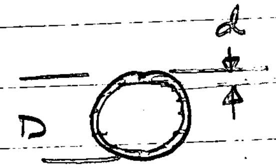

BRASS TUBING

D (ins)	d	
1.15	.04	
1.05	.04	
.87	.07	
.80	.12	(little)
.90	.04	
.78	.04	
.62	.07	
.48	.08	
.41	.04	
.45	.025	
.45	.02	

Copper wire	Brass rod	Square
.064	.065	.187
	.092	
	.123	
	.188	
	.250	

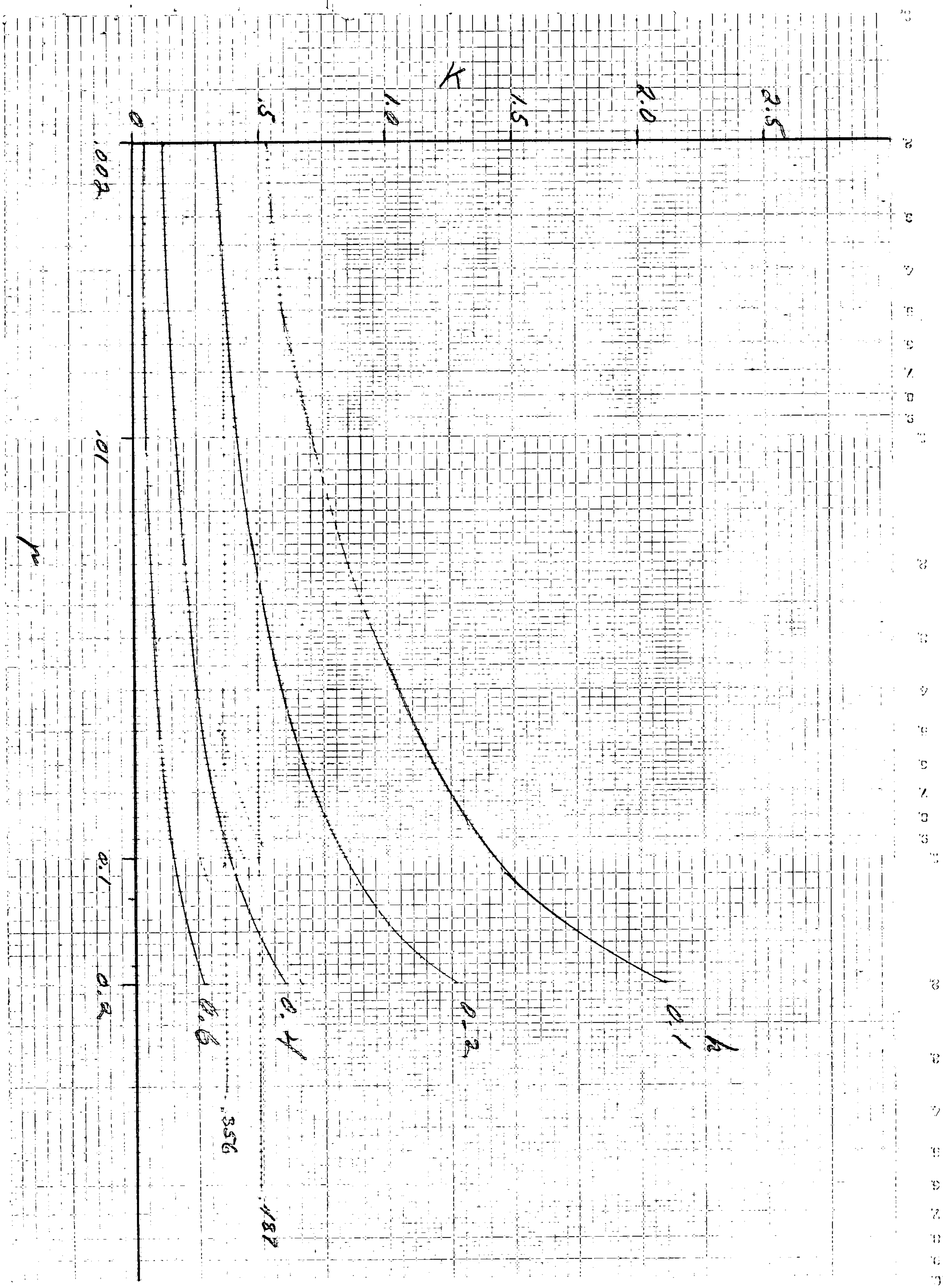
K
0
.5
1.0
1.5
2.0
2.5
.007
.01
0.1
0.2
μ
0.6
0.4
0.2
0.1
.356
.187

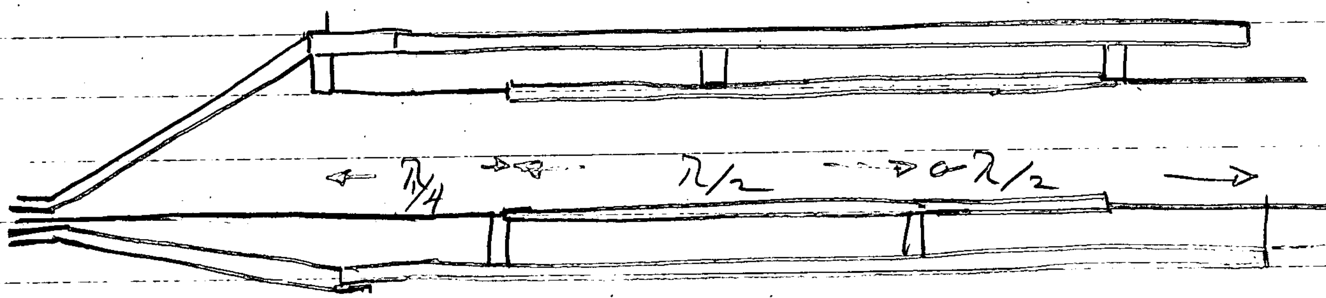

Say $h = .35$
$2r_2 = .092''$ brass
$r = .09$

then $2r_1 = (1.02'')\ 1.05''$
$2h' = .368''$

$r_1 - h' = .503 - .368$
$= .235$

$\sqrt{1.6} = 1.266$
$2 - 3.2$ kmc
$f_0 = 2.54$ kmc
$\lambda_0 = 11.8$ cm

$5/4\ \lambda_0 = 14.8$ cm
$= 5.8''$

$K = .356 = 2 \frac{\ln(a)}{\cosh^{-1}(b)}$

Say $r_2 = .064$
$r_1 = .62$ } $r = .103$

from the graph

$h = .42$
$h' = .26''$

$.62$
$.26$
$.36$

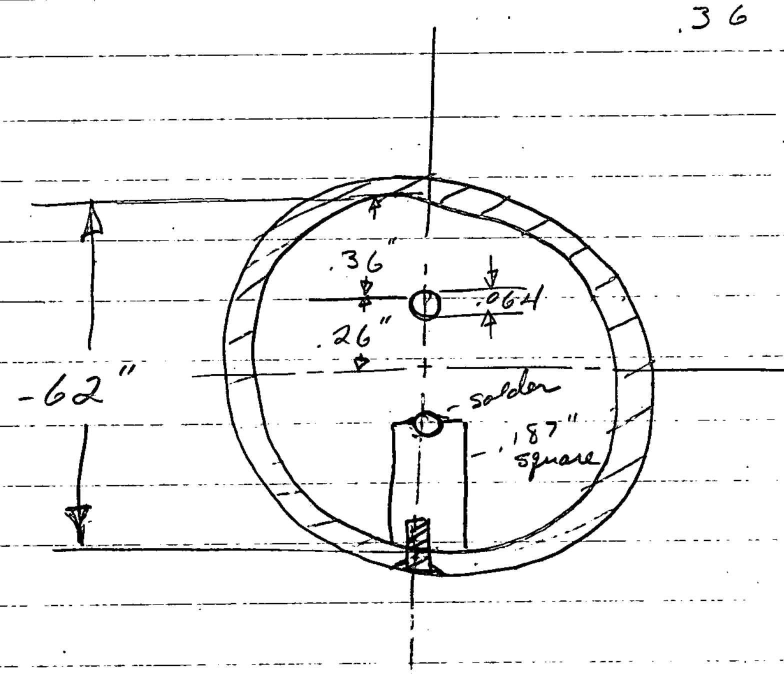

the inner conductor of 50 Ω coax is #16
or 50.8 mils

$\frac{64}{51} = 1.25$

$\frac{92}{51} = 1.8$

$$\frac{1-(k')^2}{k'} = \sqrt{\frac{1-k^2}{k}}$$

if $k = .356$

$1-(k')^2 = k' \cdot 1.565$

$(k')^2 + 1.565\,k - 1 = 0$

$k' = .487$

$$\sqrt{\frac{1-(.356)^2}{.356}}$$

$$\sqrt{\frac{.873}{.356}} = \sqrt{2.45}$$

$= 1.565$

$$k' = \frac{-1.565 \pm \sqrt{2.45+4}}{2}$$

$.975$

$$= \frac{-1.565 + 2.540}{2}$$

Graphs # 4 & 5

This data was taken to determine the application of the CLEVITE X-78C transistor (maximum dissipation 1 w) to the problem of energizing the GE microminiature relays.

Two relays are ordered. One requires 300 mw at 100 ohms and the other 150 mw at 720 ohms.

The input impedance for grounded base operation is rather low - roughly 50 ma of driving current are required to get 50 ma at the 100 Ω level. (graph # 4)

The input impedence for grounded collector operation is quite high - 11.6 volts input were required for 1 ma output at 100 Ω with 7.6 volts of collector voltage.

* Grounded emitter operation seems most desirable then. Either working directly into the 300 mw relay or through a transformer into the 150 mw relay.

ACS 21 Dec 55

#4

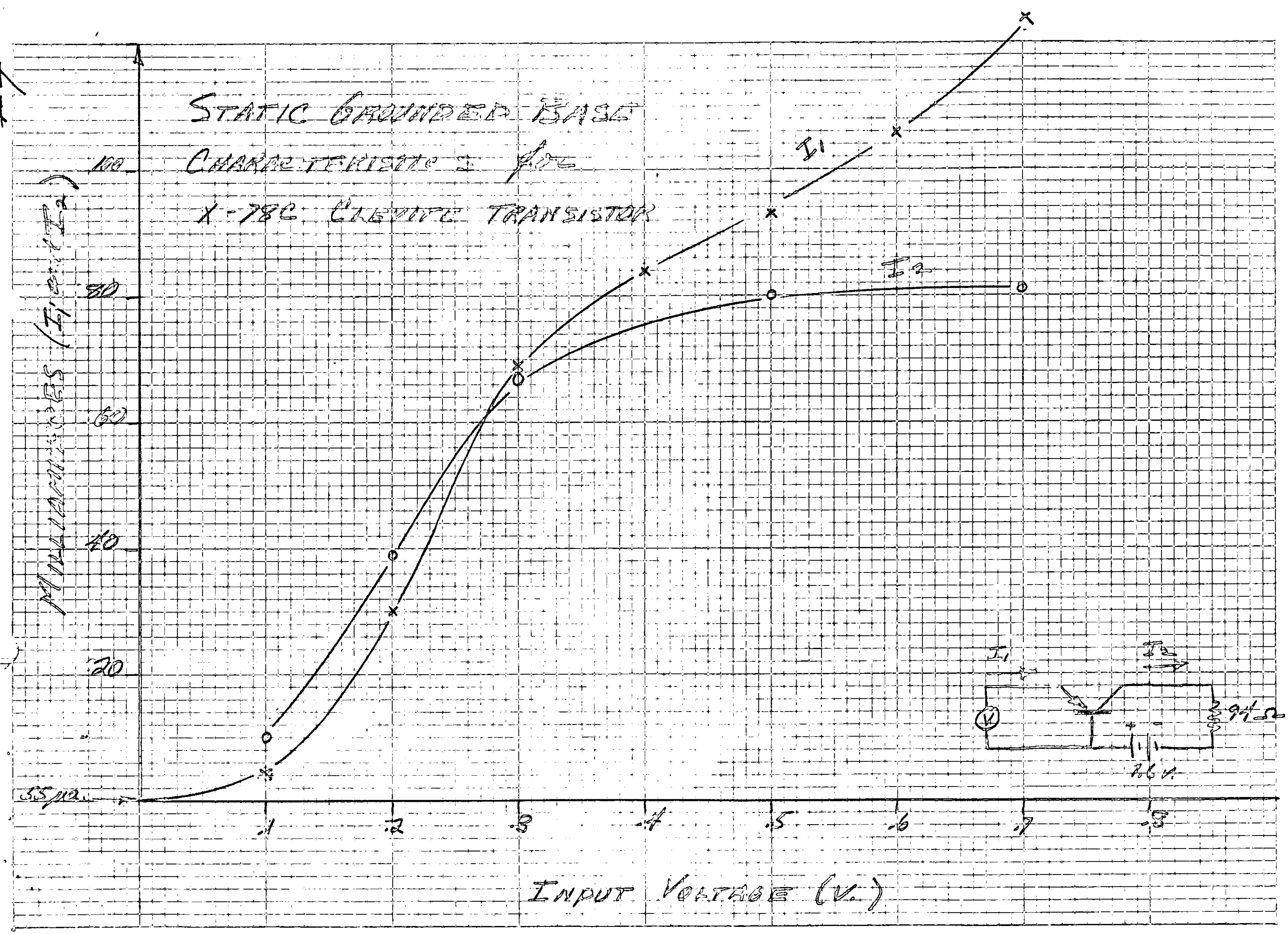
STATIC GROUNDED BASE
CHARACTERISTIC I Ac
X-78C CLEVITE TRANSISTOR
MILLIAMPERES (I_1 and I_2)
100
80
60
40
20
55 μa.
.1
.2
.3
.4
.5
.6
.7
.8
INPUT VOLTAGE (V.)
I_1
I_2
I_1
I_2
V
94 Ω
1.6 V.

#5

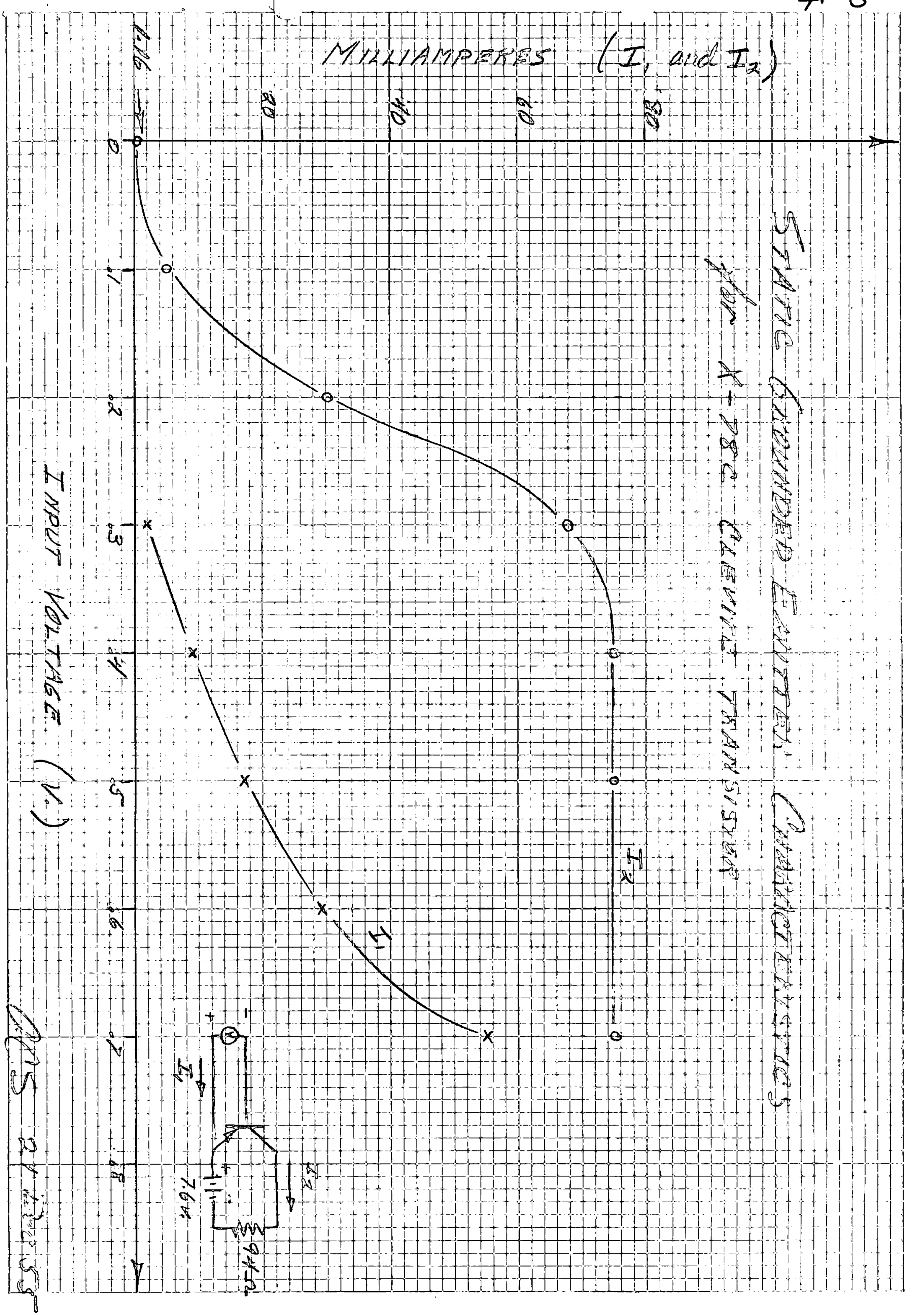

KEUFFEL & ESSER CO
10 X 10 to the inch.
MADE IN U.S.A.

#3

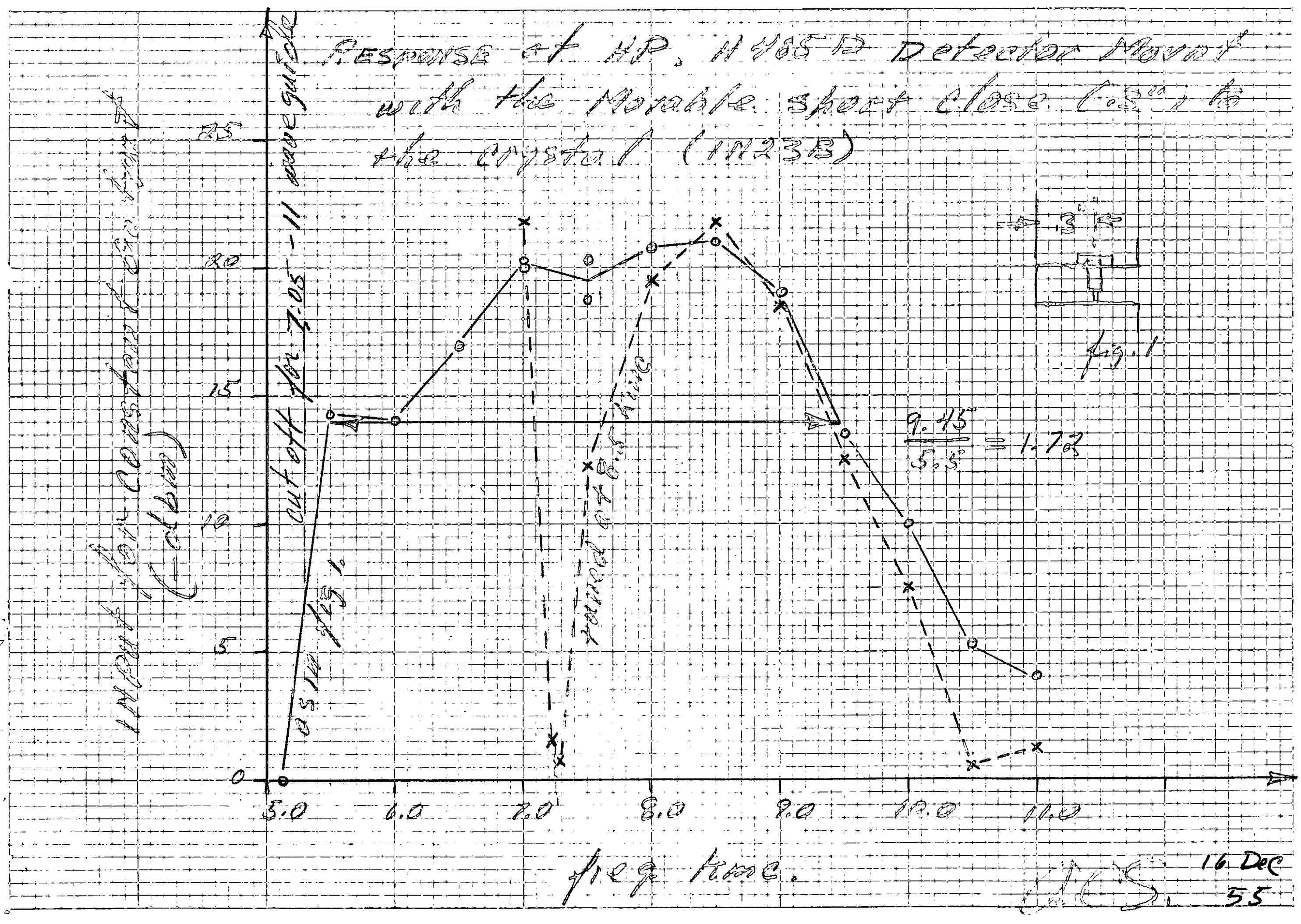
Response of H.P. H485 D Detector Mount
with the Movable short close (.3") to
the crystal (1N23B)
Input for constant o/p
(-dbm)
cut off for 7.05 - 11 wave guide
25
20
15
10
5
0
5.0
6.0
7.0
8.0
9.0
10.0
11.0
freq. kmc.
.3"
fig. 1
9.45/5.5 = 1.72
16 Dec
55

GRAPH #1 #2

This graph shows the low level response of a 1N23B crystal in the HP H485 detector mount compared with the response of the same crystal in the PRR-6 detector mount (coaxial type.)

From this two inferences might be drawn:

1) the coax type mount is more broadband than the waveguide type.

2) The useful "band width" of the H485D mount is from about 7.75 to 9.25 kmc. This is a ratio of about 1.19 in frequency. Since the $\sqrt[4]{6} = 1.595$, this indicates that a detector design similar to the H485D will not suffice for the running light.

However it should be noted that band [redacted] STAT of the PRR-6 use this type of detector.

acs 13 Dec 55

GRAPH #1

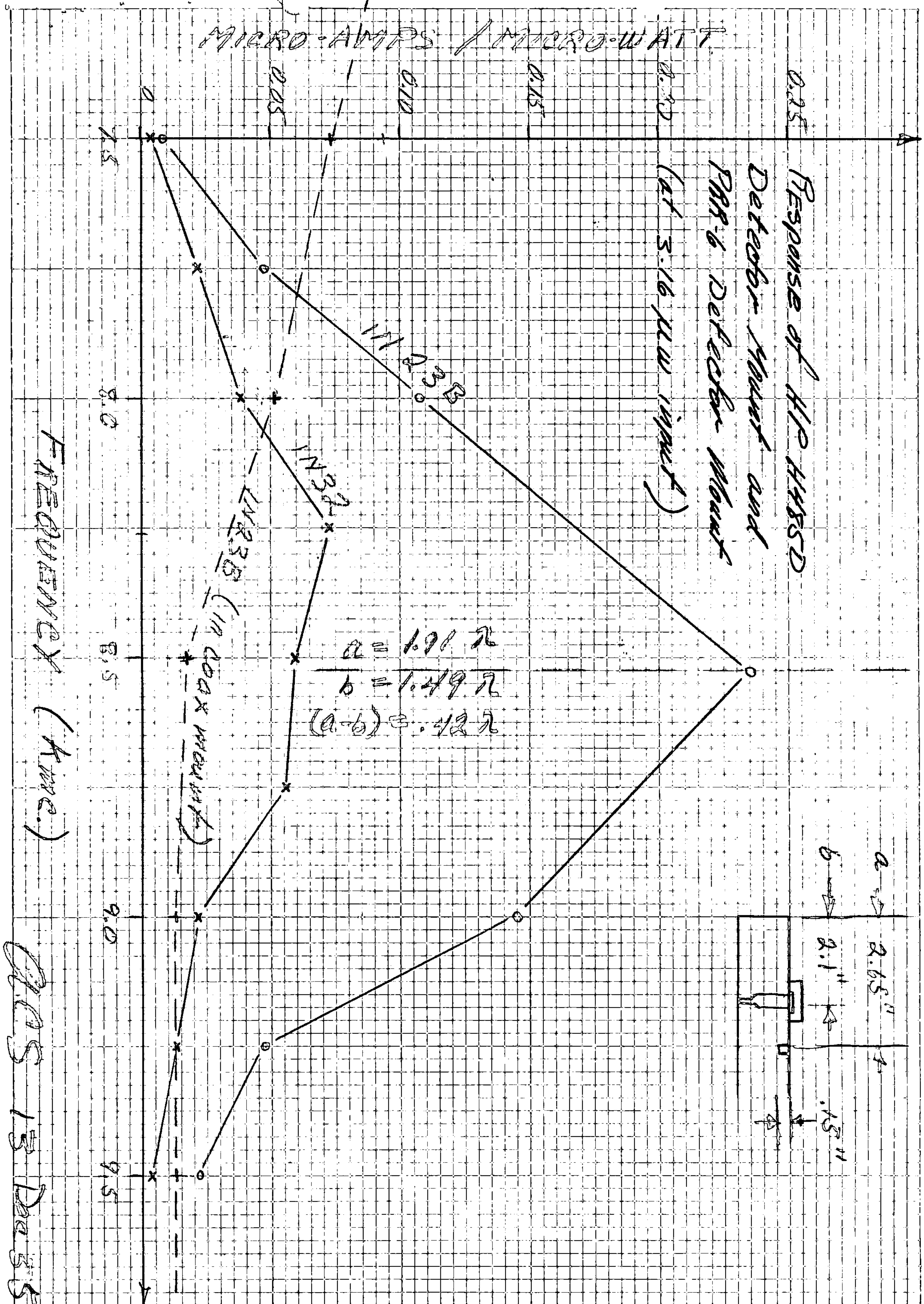

MICRO-AMPS / MICRO-WATT
0
0.05
0.10
0.15
0.20
0.25
Response of HP H485D
Detector Mount and
PRD-6 Detector Mount
(at 3.16 uw input)
1N 23B
1N32
1N23B (in coax mount)
a = 1.91 λ
b = 1.49 λ
(a-b) = .42 λ
a
b
2.65"
2.1"
.15"
7.5
8.0
8.5
9.0
9.5
FREQUENCY (Kmc)
JCS 13 Dec 55

Graph #2

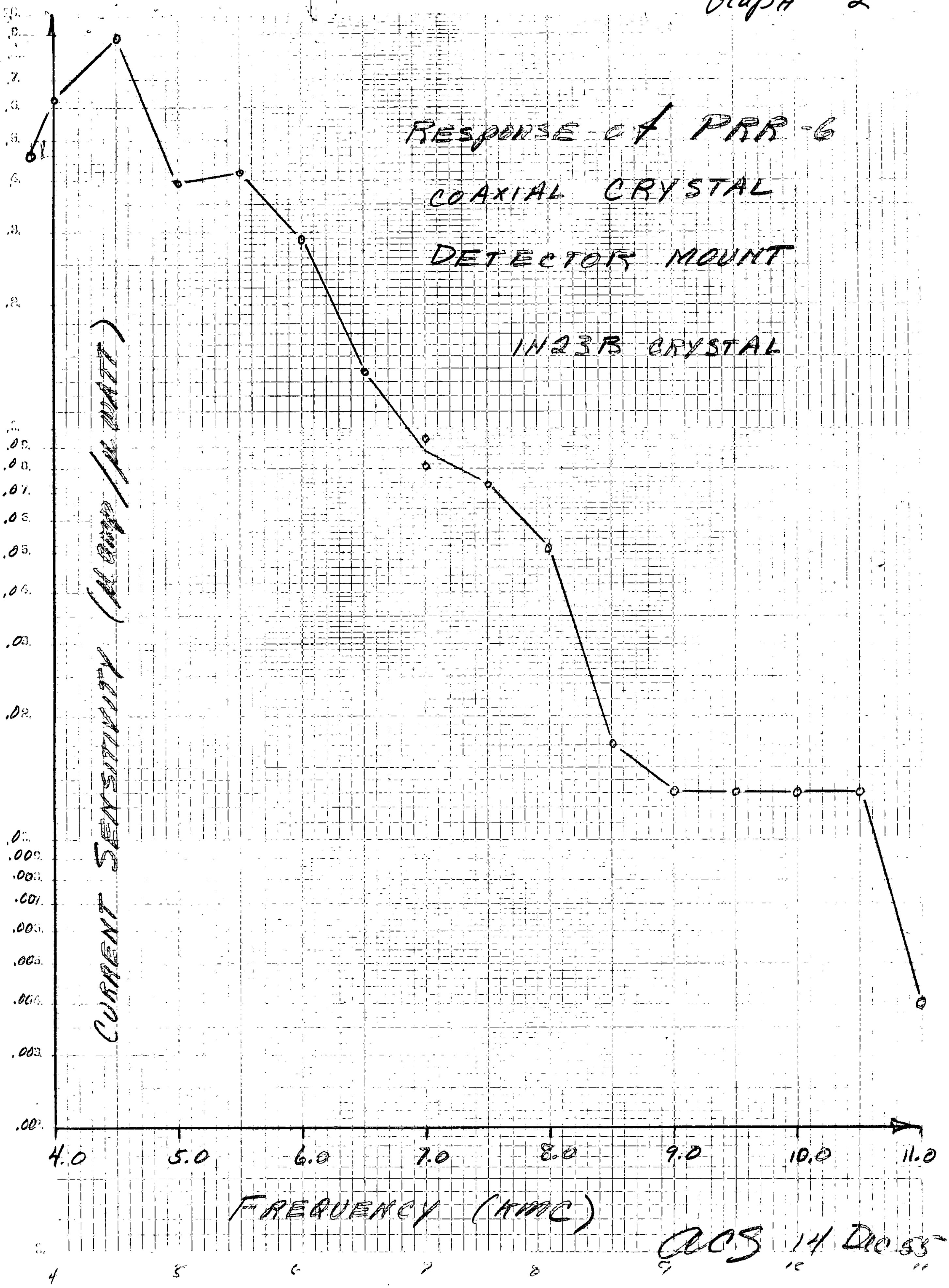

ACS 14 Dec 55

STATIC GROUNDED EMITTER CHARACTERISTICS

for MH - 2N57 TRANSISTOR

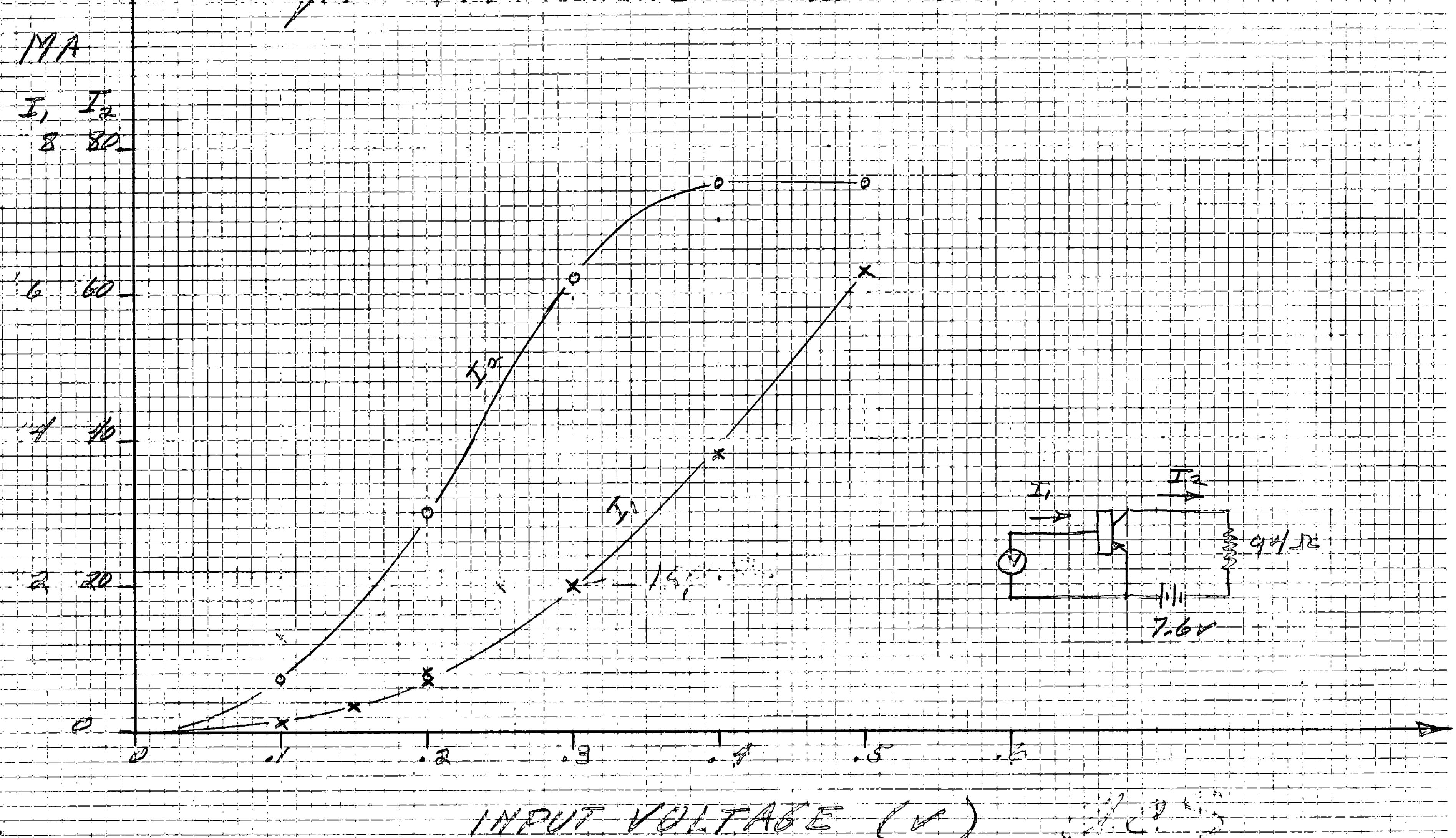

5 Jan 56

YARDNEY ELECTRIC CORPORATION
105-107 CHAMBERS STREET NEW YORK 7. N. Y.

CABLE ADDRESS:
"YARDNELECT" NEW YORK

TELEPHONE:
WORTH 2-5500

CURRENT PRICE SCHEDULE FOR THE YARDNEY SILVERCEL

May 15, 1953

TYPE*	1 – 9	10 – 99	100 – 249	250 – 499	
LR05 & LR1	$ 6.00	$ 5.50	$ 5.25	$ 5.00	Special discounts are made on orders for quantities larger than those listed herein.
HR05 & HR1	10.00	9.00	8.00	7.00	
LR3 & HR3	18.00	16.00	14.00	12.00	
LR5 & HR5	25.00	20.00	16.00	13.00	
LR10 & HR10	30.00	25.00	21.00	19.00	
LR20	40.00	36.00	32.00	30.00	
HR20	54.00	48.00	43.00	38.00	
HR21	60.00	54.00	48.00	42.00	
LR40	50.00	45.00	40.00	35.00	
HR40	100.00	90.00	80.00	70.00	
LR60	60.00	54.00	48.00	45.00	
HR60	125.00	110.00	100.00	90.00	
LR100	120.00	108.00	96.00	84.00	
HR85-HR90-HR100	150.00	120.00	110.00	100.00	

TERMS: Net 10 days, F.O.B. our plant, New York

DELIVERY: Orders for small quantities can be filled within 3 weeks from receipt of order.

NOTE: Prices and models are subject to change without notice. As production schedules increase, we anticipate that prices will be revised accordingly.

* See 1953 Brochure

OUTPUT CHARACTERISTICS

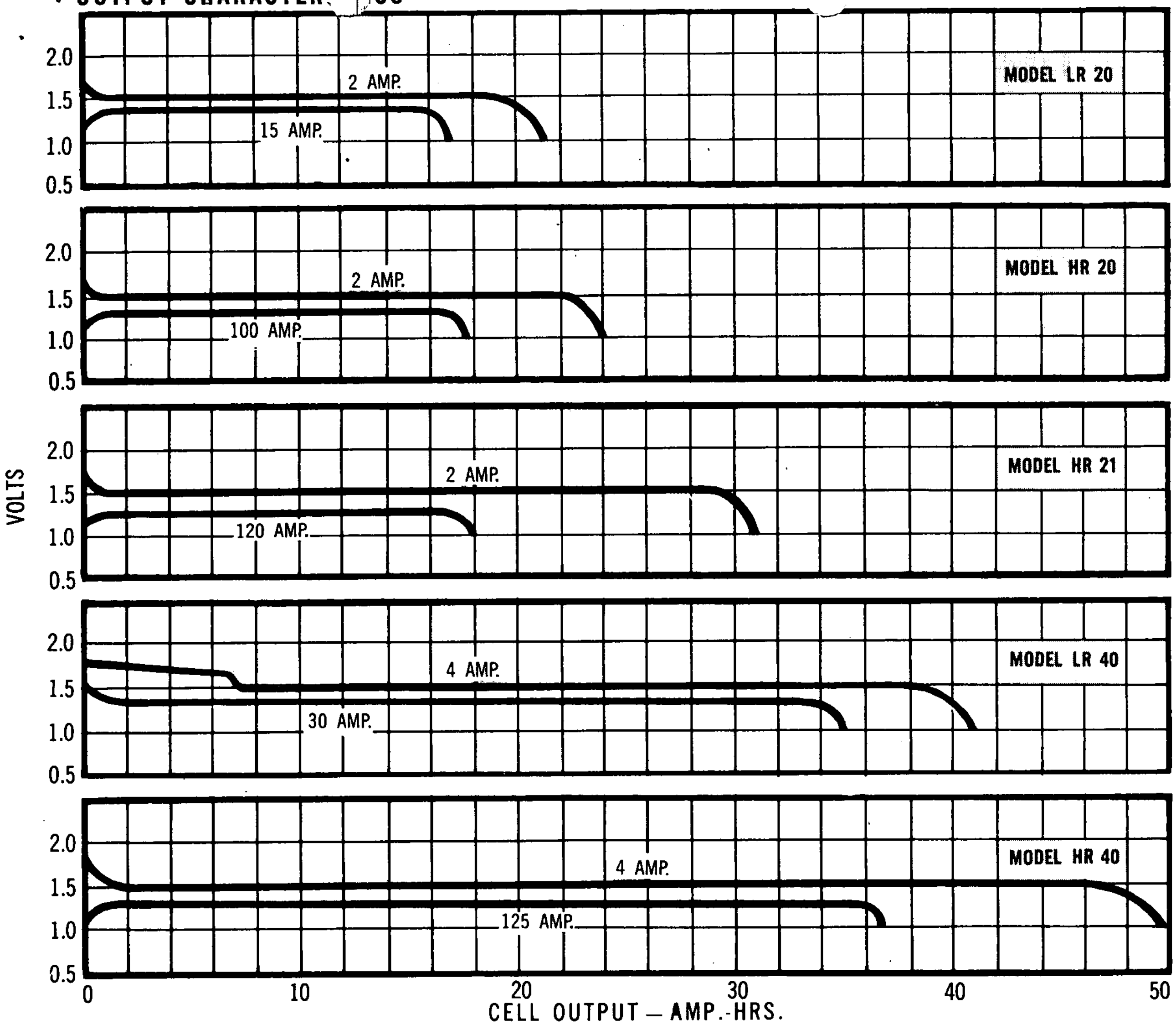

DESIGN CURVES

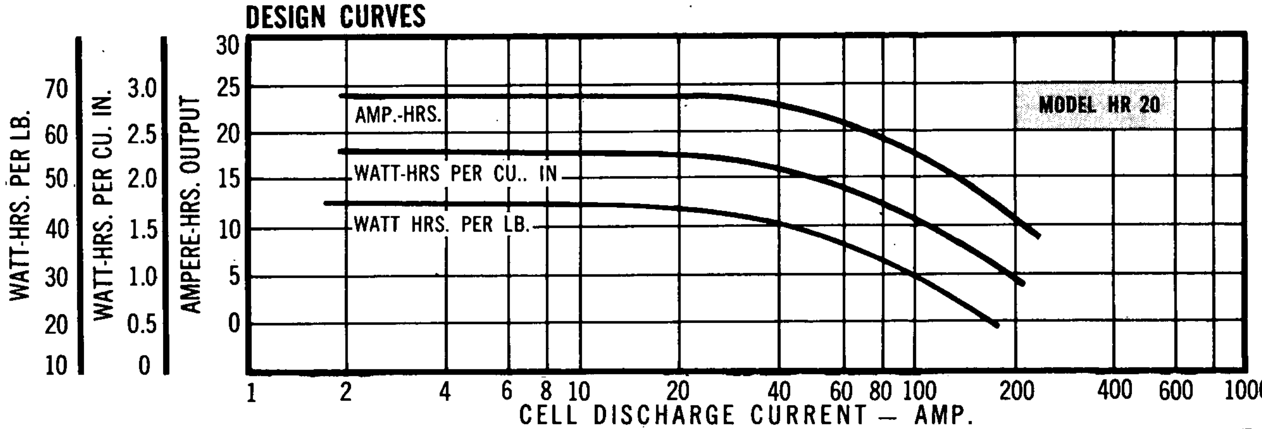

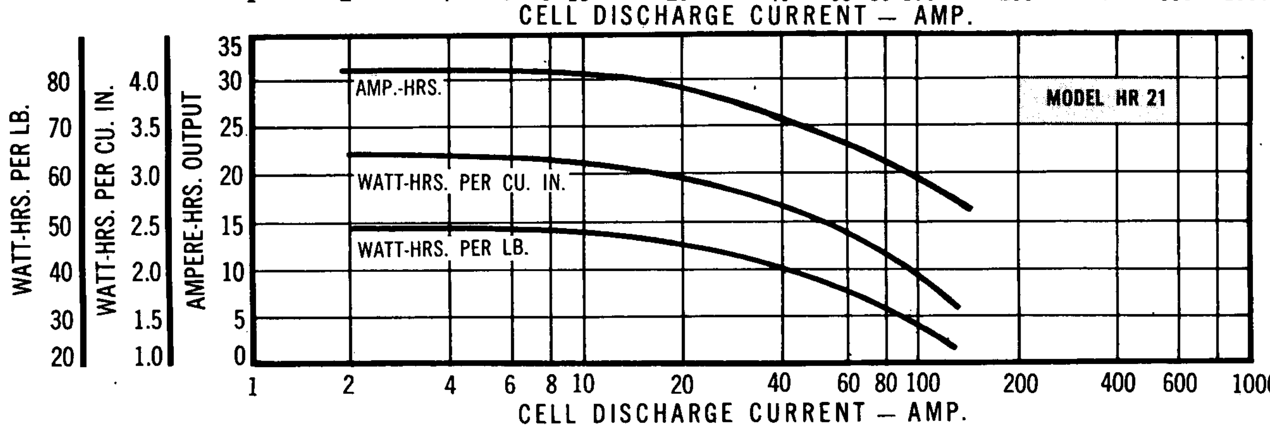

YARDNEY ELECTRIC CORP.

105-107 CHAMBERS STREET · NEW YORK 7 · N. Y.
Licensee for U.S.A. of Yardney International Corp.

1952 issue

Technical Data Sheet No. 3

CELL MODELS LR20, HR20, HR21, LR40, HR 40

formerly 20 HR 15, 20 HR-GS-BS, 20 HR-NS, 40 HR-NS

Cell Model	LR 20		HR 20		HR 21		LR 40		HR 40	
Nominal capacity — amp.-hrs.	20		20		20		40		40	
Weight (filled)-oz.	12.60		12.70		15.0		22.0		23.0	
Volume — cu. in.*	15.4		15.4		14.4		22.7		22.7	
Recommended charging cur.-amp.	1.0		2.0		3.0		2.0		3.0	
Max. continuous disch. cur.-amp.	15		100		125		40		125	
Peak discharge current-amp.	150		500		500		200		600	
Discharge current-amp.	2.0	15.0	2.0	100	2.0	120	4.0	30.0	4.0	125
Voltage **	1.51	1.40	1.51	1.35	1.50	1.35	1.50	1.40	1.51	1.35
Working capacity — amp.-hrs. †	21.0	16.7	24.0	17.7	31.0	18.0	41.0	35.0	50.0	36.8
Watt-hrs. per lb.	40.3	29.7	45.6	30.1	49.6	25.9	44.7	35.7	52.5	34.6
Watt-hrs. per cu. in.*	2.06	1.52	2.36	1.55	3.23	1.69	2.71	2.16	3.33	2.18

*Calculated using cell heights inclusive of terminals
**Voltage over flat portion of the discharge curve
† To 1 volt end point

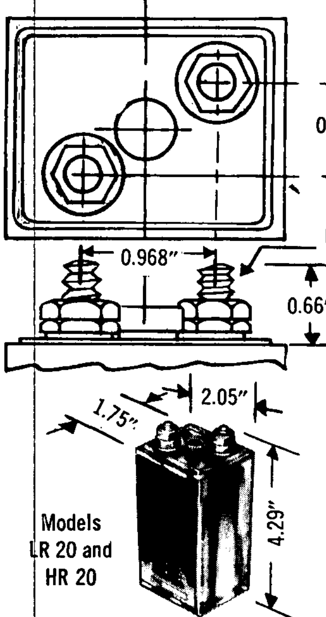

Models LR 20 and HR 20

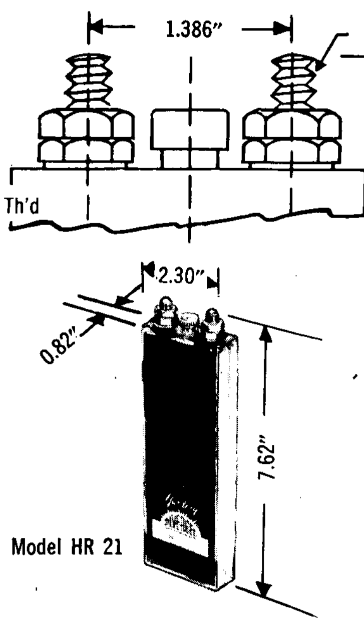

Model HR 21

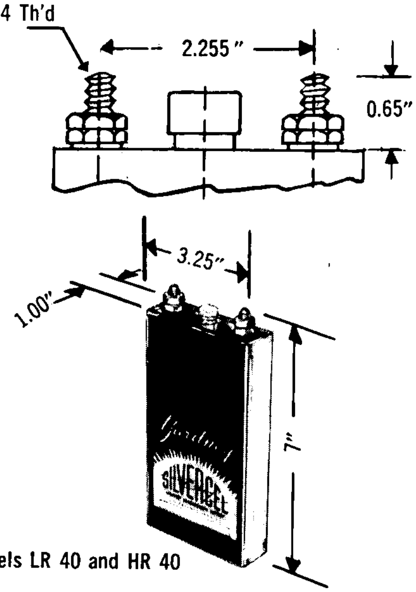

Models LR 40 and HR 40

TYPICAL DISCHARGE CURVES AT SEVERAL TEMPERATURES

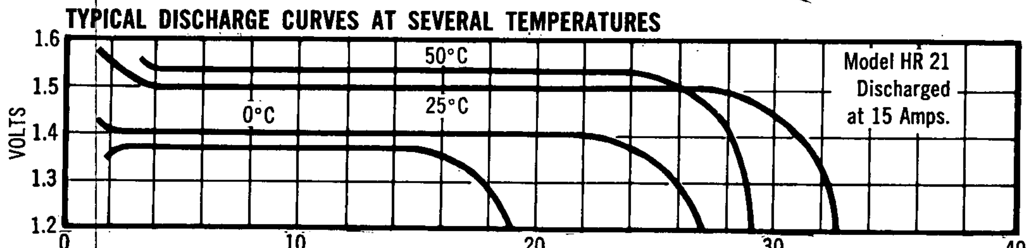

For instructions on operation, maintenance, and storage see "General Operating and Maintenance Instructions for Yardney Silvercels."

WORLD WIDE PATENTS PENDING OR GRANTED

Sheet No. 1

April 1955

APPENDIX

To General Application, Operating and Maintenance Instructions

YARDNEY ELECTRIC CORPORATION
40-46 Leonard Street
New York 13, N.Y.

OPERATING INSTRUCTIONS FOR YARDNEY SILVERCELS IN THE WET-FORMED CONDITION

Letters in parenthesis, refer to general reference table attached....................

CHARGE:

For best results, charge at a constant current rate of (**A**) until the cell/battery **voltage**, while charging, reaches (**B**) volts.

NOTE:

The voltage, **while charging,** is the indication of the state of charge of a cell **or battery**; however, nominal capacity of a fully discharged cell or battery may be **obtained by charging** at (A) current for (C) hours. Charging to the nominal capacity is not **always a complete** charge, and this method should not be used repeatedly.

CAUTION:

Continuous or repetitive overcharge will result in damage to the cell **or battery.**

LOW-RATE DISCHARGE: (For all type cells on one hour rate or longer time.)

An individual cell is considered discharged when its voltage under load **drops to one volt.** Cells assembled in a battery are considered discharged when the **overall battery voltage** under load drops below the number of cells in the battery **multiplied by one volt.**

HIGH-RATE DISCHARGE: (HR-V* and HR Cells only on less than one hour rates.)

When discharging at high rates, **discharge time limitations** should be **observed or cells** may overheat, **resulting in** distortion of cell cases and shortening of life. [redacted]

[redacted]

ELECTROLYTE – AS APPLICABLE FROM THE REFERENCE TABLE

If the electrolyte level of a cell is at the minimum height (D), immediately **after charge,** some distilled water should be added to bring the level to the **correct height as shown** in (E) of the reference table. The addition of distilled water, **when required, may be accomplished** by removing the plastic vent cap and the sponge rubber **plug from the vent hole** of the cell and adding water by means of a syringe. **Extreme caution should be taken to** prevent damage to the cell electrodes or separator by the tip of the syringe.

For additional information refer to General Application, Operating and **Maintenance** Instructions issued November 1953 – Technical Data Sheet No. 101

*FORMERLY DESIGNATED AS MR CELLS

SILVERCEL
REG. U.S. PAT. OFF.

ebruary 1956

Sheet No. 2A

YARDNEY ELECTRIC CORPORATION

40-46 LEONARD STREET NEW YORK 13. N. Y.

GENERAL REFERENCE TABLE – (MEDIUM-RATE CELLS) (HIGH-RATE CELLS)

CELL TYPE MR = Medium Rate HR = High Rate	HR05	HR1	HR3	HR5	MR12	MR100	HR10	HR20	HR21	HR40	HR60	HR85	HR90	HR100
A*1 Optimum Current (Amperes) Single Cell Battery	.07 .07	.12 .10	.40 .30	.50 .35	1.0 1.0	6 5	1.0 1.0	3.0 2.0	3.0 3.0	4 3	6 4	10 6	10 6	10 6
B*2 Maximum single cell voltage while charging	2.0	2.0	2.0	2.0	2.1	2.1	2.0	2.0	2.0	2.0	2.0	2.0	2.0	2.0
C Hours Single Cell Battery	7 7	8 10	8 10	10 14	12 12	16 20	10 10	7 10	7 7	10 13	10 15	8 14	9 15	10 16
D*3 Minimum Level of electrolyte	¼	¼	¼	½	½	1	No additional electrolyte or distilled water is required during normal life of this type cell.							
E*3 Normal Level of electrolyte	½	¾	1"	1	1½	2								
F Time Limitation factor	1.0	2.0	4	8	12	100	10	20	25	40	60	85	90	100

*1 These current rates are generally based on a 10-20 hour charge. Cells may be charged at higher current rates whenever necessary. However, caution must be taken not to exceed the final voltage, **while charging in B** above, or an increase in cell temperature above 120-130°F during charge. **A charging current of the one hour rate is permissible**; for specific informations contact Manufacturer.

*2 Any battery is fully charged when its voltage, **while charging,** equals the number of cells in the battery multiplied by 2.0 volts. (Tolerance = ± 1.5% of the overall battery voltage)

*3 Electrolyte level heights (shown in (D) and (E) above) are measured in inches from the bottom of cells **immediately** after charge.

A Coupled "Coaxial" Transmission-Line Band-Pass Filter*

J. J. KARAKASH†, ASSOCIATE, IRE, AND D. E. MODE‡, SENIOR MEMBER, IRE

Summary—Band-pass filters employing tuned coupled circuits are used to advantage at low frequencies and, because they have good electrical characteristics, it may be desirable to adapt them to the very-high frequencies. However, at frequencies bordering on the microwave region, it is no longer possible to treat such circuit elements in the usual low-frequency fashion, the distributed character of the parameters becoming of prime importance. This paper describes a band-pass filter in which the coupled elements consist of a shielded pair of cylindrical conductors. Because the analysis is based upon transmission line theory, the results are valid and usable at microwave frequencies until transmission other than the *TEM* mode becomes troublesome.

* Decimal classification: R386.1. Original manuscript received by the Institute, January [illegible], 1949; revised manuscript received, August 3, 1949. This work was done under contract W28 [illegible] 128 between the Air Matériel Command, Watson Laboratories, and Lehigh University.

† Lehigh University, Bethlehem, Pa.

I. Introduction

Coupled tuned circuits have long been used as band-pass filters for they may be designed to give satisfactory performance in both the pass band and in the adjacent stop bands. An attempt to design such filters for use at microwave frequencies finds the elements involved reduced to little more than leads, and a transmission-line approach to the problem must, therefore, be made if a design is to be anything more than a "cut and try" process.

An elementary mechanical layout of the coupled transmission-line band-pass filter to be discussed is shown in Fig. 1. The tuned circuits are the transmission lines and the coupling is that existing between them. Radiation losses are eliminated due to the shield; in this sense, the system will be referred to as a coaxial filter.

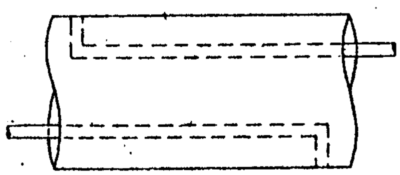

Fig. 1—Elementary prototype section of a coupled "coaxial" transmission-line band-pass filter.

II. Transmission in a Coupled "Coaxial" System

Equations for the current and voltage functions along two identical mutually coupled transmission lines such as shown in Fig. 2 have been presented by Fuchs.[1]

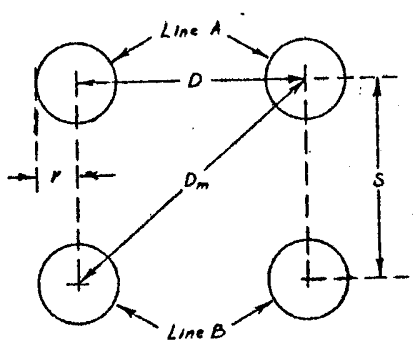

Fig. 2—A balanced coupled "coaxial" transmission line, in cross section.

These are

$$E_A = a_1\epsilon^{j\beta l} + b_1\epsilon^{-j\beta l} \tag{1}$$

$$E_B = a_2\epsilon^{j\beta l} + b_2\epsilon^{-j\beta l} \tag{2}$$

$$I_A = \frac{Z_0a_1 - Z_ma_2}{Z_0^2 - Z_m^2}\epsilon^{j\beta l} - \frac{Z_0b_1 - Z_mb_2}{Z_0^2 - Z_m^2}\epsilon^{-j\beta l} \tag{3}$$

$$I_B = \frac{Z_0a_2 - Z_ma_1}{Z_0^2 - Z_m^2}\epsilon^{j\beta l} - \frac{Z_0b_2 - Z_mb_1}{Z_0^2 - Z_m^2}\epsilon^{-j\beta l} \tag{4}$$

in which the subscripts A and B serve to identify the transmission lines, l is the line length, Z_0 is the characteristic impedance of either line alone, Z_m is the mutual impedance between lines, and a_1, b_1, a_2, and b_2 are constants. For the system shown in Fig. 2,

$$Z_0 = 120 \log_\epsilon \frac{D}{r}$$

$$Z_m = 120 \log_\epsilon \frac{D_m}{S} \tag{6}$$

neglecting proximity effects and assuming perfect conductors.

Equations (1) through (4) may be applied to the balanced coupled coaxial transmission-line system shown in cross section in Fig. 3 if Z_0 and Z_m are properly interpreted.

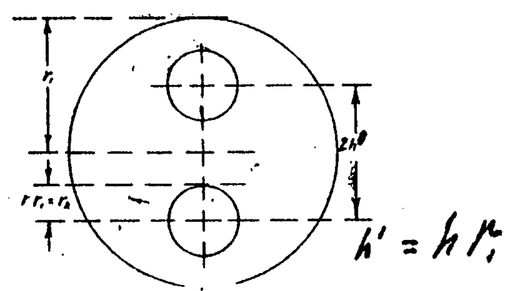

Fig. 3—Cross section of two parallel open-wire transmission lines.

In order to derive the required relations, McCracken[2] has utilized the bilinear transformation

$$W = \frac{aZ + b}{cZ + d} \tag{7}$$

evaluating the complex constants a, b, c, and d so that the configuration in the Z plane shown in Fig. 4(b) transforms, in the W plane, to the arrangement of Fig. 4(a). The large circle in the Z plane becomes the u axis in the W plane. Electrically, therefore, the bilinear transformation converts the dual coaxial line into an equivalent open-wire pair. Using the method of images, the conducting plane may be replaced by the two conductors shown below the u axis in Fig. 4(a), so that the system has the same geometry as that of Fig. 2. From (6) with the appropriate dimensions obtained from Figs. 2, 3, and 4(a), there results, using transformation (7),

[1] Morton Fuchs, "Intercoupled transmission lines at radio frequencies," *Elec. Commun.*, vol. 21, no. 4, pp. 248–256; 1944.

[2] L. G. McCracken, Unpublished Master's Thesis, Lehigh University, June, 1947.

$$Z_m = 120 \log_e \frac{1 + h^2 + r^2}{2h}. \tag{8}$$

The expression for Z_0 is had by calculating the capacitance C (per unit length) of two eccentric cylinders one within the other and utilizing the relations,

$$L = \frac{1}{Cc^2}$$
$$Z_0 = \sqrt{\frac{L}{C}} \tag{9}$$

where

L = the inductance of the line per unit length

c = the velocity of light.

The result is

$$Z_0 = 60 \cosh^{-1} \frac{1 - h^2 + r^2}{2r}. \tag{10}$$

The electrical performance of a coupled coaxial system (Fig. 3) is then expressible in terms of (1) through (4), with Z_m and Z_0 coming from (8) and (10).

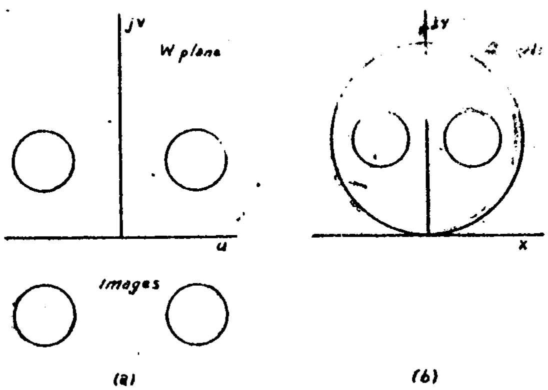

Fig. 4—Illustrating the complex transformation from a coaxial to an open-wire system.

III. General Properties of the Coupled Transmission-Line Filter

Calling the electrical length of the filter $\theta = \beta l$, using the defining equations (11) and (12),

$$E_s = AE_L + BI_L \tag{11}$$

$$I_s = CE_L + DI_L \tag{12}$$

the parameters A, B, C, and D for conditions shown in Fig. 5 are,

$$A = -\frac{1}{K}\cos\theta \tag{13}$$

$$B = -j\frac{Z_0}{K}(1 - K^2)\sin\theta \tag{14}$$

$$C = \frac{j \csc\theta(\cos^2\theta - K^2)}{Z_0(1 - K^2)K} \tag{15}$$

$$D = A \tag{16}$$

in which

$$K = \frac{Z_m}{Z_0}. \tag{17}$$

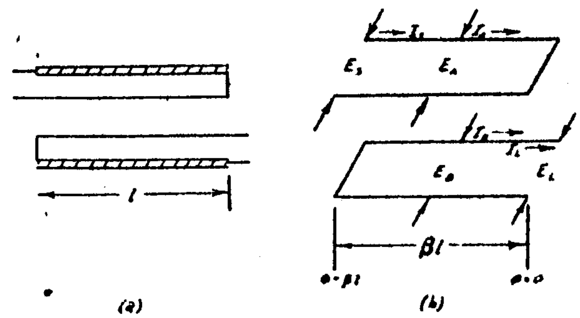

Fig. 5—A typical "coaxial" coupled transmission-line filter section. A cross section is shown in (a) and an electrical equivalent in (b).

The characteristics of the filter may be summarized as follows:

1. The pass band (defined for real Z_I) occurs for

$$1 \leq A = -\frac{1}{K}\cos\theta \leq 1 \tag{18}$$

giving the cutoff conditions,

$$\theta = \cos^{-1}(\pm K) \tag{19}$$

from which it is seen that the pass-band center frequency f_0 occurs where the lines are one-quarter wavelength long, the width of the pass band depending upon the parameter K.

2. The reactive attenuation in the stop bands is, in nepers,

$$\alpha = \cosh^{-1}\left|\frac{\cos\theta}{K}\right|. \tag{20}$$

3. The normalized image impedance of the filter is given by,

$$\frac{Z_I}{Z_0} = (1 - K^2)\sqrt{\frac{\sin^2\theta}{K^2 - \cos^2\theta}}. \tag{21}$$

At the midband frequency f_0 (an important point from the standpoint of impedance matching), this is,

$$\left.\frac{Z_I}{Z_0}\right]_{f_0} = \frac{1 - K^2}{K} \tag{22}$$

which reduces to unity for $K = 0.619$.

The general form of the attenuation and image-impedance functions is shown in Figs. 6 and 7, respec-

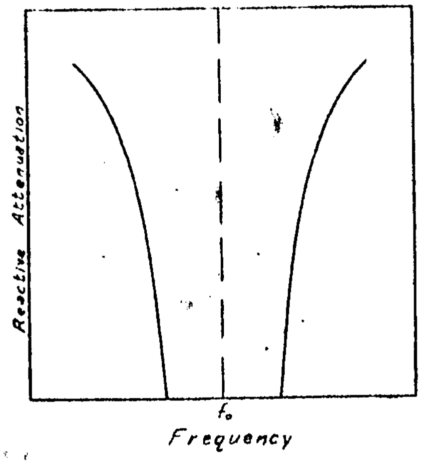

Fig. 6—Typical reactive attenuation of a coupled "coaxial" transmission line filter.

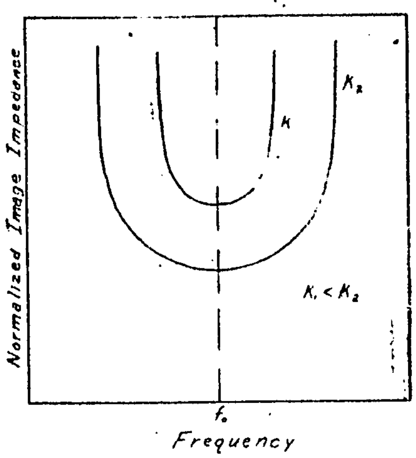

Fig. 7—Image-impedance behavior of a coupled "coaxial" transmission-line filter, K as parameter.

tively. Certain similarities in the electrical performance of the coupled coaxial transmission-line filter and its lumped-element predecessor are worthwhile pointing out. An equivalent circuit of a lumped-element coupled circuit filter is shown in Fig. 8. Assuming lossless circuit

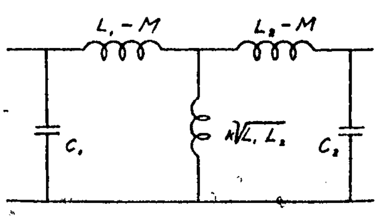

Fig. 8—An equivalent circuit of a lumped-element coupled circuit band-pass filter.

elements, that the coupled circuits are tuned to the same frequency f_0, and that $L = L_1 = L_2$, the image impedance of this filter (normalized to $Z = \sqrt{L/C}$) is

$$\frac{Z_I}{Z} = \sqrt{\frac{(1-k^2)(f_0/f)^2}{\left[(1-k) - \frac{f_0^2}{f^2}\right]\left[\frac{f_0^2}{f^2} - (1+k)\right]}} \tag{23}$$

a typical plot of which is shown in Fig. 9. The bandwidth (defined for real Z_I) may be written,

$$BW = \frac{\omega_0}{\sqrt{1-k}} - \frac{\omega_0}{\sqrt{1+k}}. \tag{24}$$

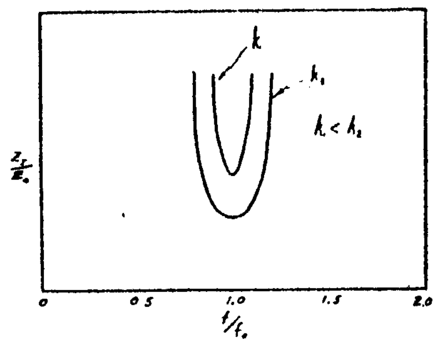

Fig. 9—Image-impedance characteristics of the lumped-element filter shown in Fig. 8.

Comparison with the coupled transmission-line filter shows that the image-impedance curves have similar form and the bandwidth is dependent upon k or K in a similar manner, becoming zero when $k = K = 0$.

IV. The Reduction of Reflection Losses

In order that the insertion loss in the filter pass band be small, the filter image impedance should match that of the circuit in which it is to work. Equation (21) shows that there are three parameters in the image-impedance equation, θ, K, and Z_0. Only two of these are independent, however, and these are required for fixing the bandwidth and center frequency of the filter. Another parameter must be introduced, therefore, so that the nominal impedance of the filter be adjustable to an optimum value. The familiar quarter-wave transformer matching scheme is therefore proposed.

Suppose that a coupled coaxial transmission-line filter has been designed so that its center frequency and bandwidth are the required ones. Such a filter is sketched in Fig. 10(a). Terminating sections are then added as

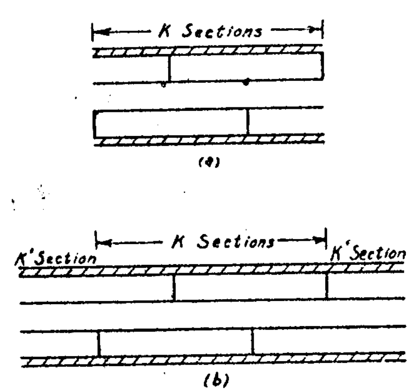

Fig. 10—The coupled "coaxial" transmission-line filter shown in cross section. (a) indicates typical midsections, and (b) shows a filter including terminating K' sections.

shown in Fig. 10(b); the K parameter (referred to as K') of these sections being chosen so that at $f = f_0$

$$Z_I' = \sqrt{Z_I Z_c} \tag{25}$$

where the prime indicates the image impedance of the terminating section, and Z_c is the external circuit impedance. If $Z_c = Z_0$, (a limiting case)

$$\frac{1 - K'^2}{K'} = \sqrt{\frac{1 - K^2}{K}}. \tag{26}$$

Two methods for the mechanical design of terminating sections are available, the first employing inner conductors of different diameter and the second a change in the eccentricity. Mechanically, the latter method is more difficult to achieve than the former. For practical narrow-band filters, $K < 0.619$ and therefore K' will be larger. For K equal to 0.619, no impedance transformation is necessary assuming $Z_c = Z_0$.

The effect of the terminating sections upon the overall image-impedance characteristic is important. A typical characteristic is shown in Fig. 11 for a single K section with two K' terminating sections.

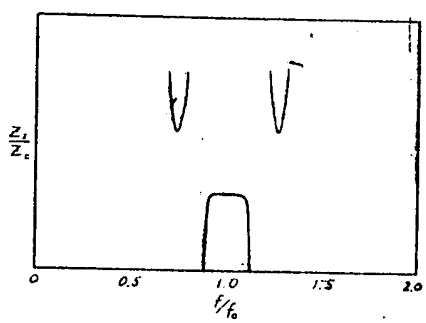

Fig. 11—Normalized image-impedance behavior of a coupled transmission-line filter having one K section together with terminating K' sections.

V. Experimental Results

As an experimental check on the theory presented, two filter models have been built and tested. The first of these had a midband frequency of 2,000 Mc, with a K of 0.44 and a K' of 0.55. The cutoff frequencies were calculated to be 2,590 and 1,410 Mc. A curve of the insertion loss *versus* frequency for this filter is shown in Fig. 12.

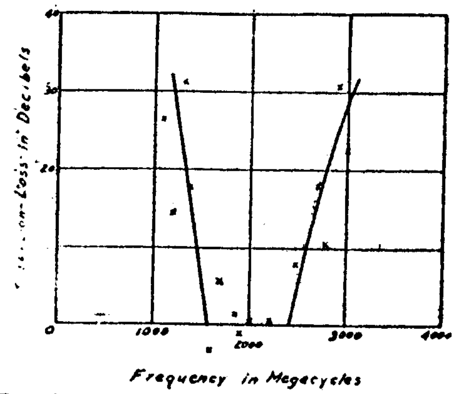

Fig. 12—Experimental insertion loss curve for a coupled transmission-line filter having parameters $f_0 = 2{,}000$ Mc, $K = 0.44$, and $K' = 0.55$.

A second filter model having a K value of 0.31 and no terminating sections was constructed for a center frequency of 1,000 Mc and a pass band between 800 and 1,200 Mc. The experimental insertion loss curve for this filter is shown in Fig. 13, where it may be seen that the

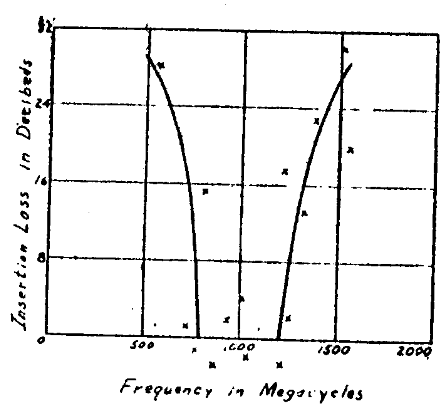

Fig. 13—Experimental insertion loss curve for a coupled transmission line filter having parameters $f_0 = 1{,}000$ Mc, $K = 0.31$.

cutoff frequencies tend to agree, but that the pass-band insertion loss is rather high. Without the terminating sections, the impedance match is rather poor, and this may explain the loss peaks in the pass band.

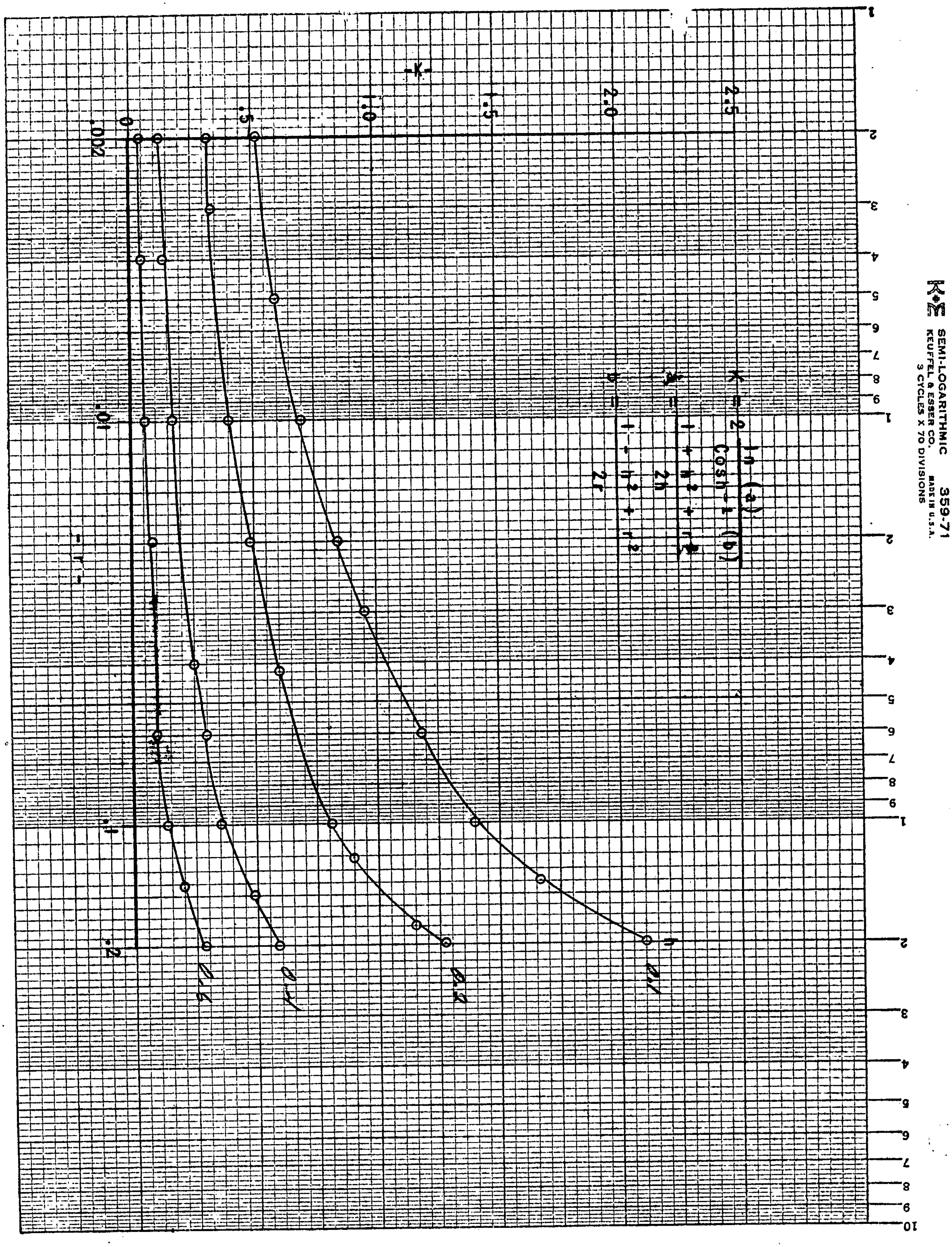
-K-
-r-
K = 2 ln (a) / cosh⁻¹ (b)
a = (1 + h² + r²) / 2h
b = (1 − h² + r²) / 2r
0.1
0.2
0.4
0.6
SEMI-LOGARITHMIC 359-71
KEUFFEL & ESSER CO. MADE IN U.S.A.
3 CYCLES X 70 DIVISIONS